Trithiocarbonates as a Novel Class of HDAC Inhibitors: SAR Studies, Isoenzyme Selectivity, and Pharmacological Profiles

Florian Dehmel,[‡] Steffen Weinbrenner,[†] Heiko Julius,[†] Thomas Ciossek,[§] Thomas Maier,[†] Thomas Stengel,[†] Kamal Fettis,[†] Carmen Burkhardt,[†] Heike Wieland,[†] and Thomas Beckers*,[ǁ]

*Nycomed GmbH, Therapeutic Area Oncology, Byk-Gulden-Strasse 2, D-78467 Konstanz, Germany*

Received January 30, 2008

Inhibitors of histone deacetylases (HDAC) are currently developed for the treatment of cancer. These include compounds with a sulfur containing head group like depsipeptide, alkylthiols, thiocarboxylates, and trithiocarbonates with a carbonyl group in the α-position. In the present investigation, we report on the synthesis and comprehensive SAR analysis of HDAC inhibitors bearing a tri- or dithiocarbonate motif. Such trithiocarbonates are readily accessible from either preformed or in situ prepared α-halogenated methylaryl ketones. A HDAC isotype selectivity and a substrate competitive mode-of-action is shown for defined analogues. Exploration of the head group showed the necessity of the dithio-α-carbonyl motif for potent HDAC inhibition. Highly potent, substrate competitive HDAC6 selective inhibitors were identified (12ac:IC_{50} = 65 nM and K_i = 110 nM). Trithiocarbonate analogues with an aminoquinoline-substituted pyridinyl-thienoacetyl cap demonstrate a cytotoxicity profile and potency comparable to that of suberoylanilide hydroxamic acid (SAHA) as an approved cancer drug.

Introduction

Posttranslational modification of proteins by reversible lysine acetylation is one important modification modulating protein function.[1] The modification of core histone proteins H3 and H4 by acetylation of *N*-terminal lysine residues is well described and part of the so-called histone code important in epigenetic processes.[2] Nevertheless, a raising number of nonhistone proteins modified by lysine acetylation have been reported, including the signal transducer and activator of transcription 1 and 3 (STAT1, STAT3),[a] heat shock protein 90 (Hsp90), the tumor suppressor protein p53, and α-tubulin.[3] The status of H3/H4 core histone acetylation correlates with the transcriptional activity of chromatin with histone acetyltransferases (HATs) and histone deacetylases (HDACs) as key players regulating reversible histone acetylation.[1b] Up to now, 11 different HDAC isoenzymes belonging to the class I (HDAC 1, 2, 3, 8), class II (HDAC 4−7, 9, 10), and class IV (HDAC11) family have been described.[4] There is clear evidence for a pathophysiological relevance of HDAC mediated histone acetylation and cancer.[5] These include (i) mutations of cAMP binding protein (CBP) as a HAT are associated with Rubinstein−Taybi syndrome, a cancer predisposition,[6] (ii) aberrant recruitment of HDAC1 by
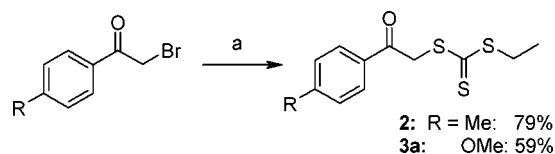
transcription factors in acute promyelocytic leukemia (APL) mediated by the PML-retinoic acid receptor α fusion gene in non-Hodgkin lymphoma by the overexpressed BCL6 protein and in acute myelogenous leukemia (AML M2 subtype) by the AML-ETO fusion protein,[7] (iii) overexpression of HDAC2 in colon carcinoma upon constitutive activation of the wnt/β-catenin/TCF signaling pathway,[8] and finally (iv) a high expression of HDAC1, 2, and 3 in gastric, prostate, and colorectal cancer correlating with survival and staging.[9] As a consequence, the identification of HDAC inhibitors is currently one major topic in oncology drug discovery programs. Inhibition of HDAC class I/II enzymes is well established as an experimental clinical approach for solid and hematological tumor therapy.[4b,10] HDAC inhibitors affect the transcriptional regulation and induce or repress genes involved in differentiation, proliferation, cell cycle regulation, protein turnover, and apoptosis.[4b] HDAC inhibitors of divergent chemical structure are currently in clinical development.[11] These include short chain fatty acids, hydroxamic acids, cyclic tetrapeptides/peptolides, ketones, and benzamides.[12] Various agents are currently in clinical development, namely the hydroxamate analogues (*E*)-3-(4-(((2-(1*H*-indol-3-yl)ethyl)(2-hydroxyethyl)amino)methyl)phenyl)-*N*-hydroxyacrylamide (LBH589), *N*-hydroxy-3-(3-(*N*-phenylsulfamoyl)phenyl)acrylamide (PXD101, Belinostat), *N*-(2-(4-(hydroxycarbamoyl)phenoxy)ethyl)-3-(isopropyl-amino)benzofuran-2-carboxamide (PCI024781) and N^1-hydroxy-8--phenyloctanediamide (suberoylanilide hydroxamic acid/SAHA, Vorinostat), the benzamide analogues (4-(2-aminophenylcarbamoyl)-benzylamino)methyl nicotinate (MS275 or SNDX275) and *N*-(2-aminophenyl)-4-((4-(pyridin-3-yl)pyrimidin-2-ylamino)methyl)-benzamide (MGCD0103), the cyclic peptolide depsi-

Scheme 1[a]

2: R = Me: 79%
3a:　　OMe: 59%

[a] Reagents and conditions: (a) EtSNa, CS_2, THF, rt.

---

* To whom correspondence should be addressed. Phone: +761-5155916. Fax: +761-5155595. E-mail: Thomas.Beckers@oncotest.de. Address: Oncotest GmbH, Institute for Experimental Oncology, Am Flughafen 12−14, D-79108 Freiburg, Germany.

† Nycomed GmbH, Therapeutic Area Oncology.
‡ Present address: Henkel KGaA, D-40589 Düsseldorf, Germany.
§ Present address: Boehringer Ingelheim Pharma.
ǁ Present address: Oncotest GmbH, Institute for Experimental Oncology.

[a] Abbreviations: APL, acute promyelocytic leukemia; AML, acute myelogenous leukemia; AMC, 7-amino-4-methylcoumarin; ATCC, American Tissue Type Collection; CBP, cAMP binding protein; CTCL, cutaneous T-cell lymphoma; FACS, flourescence activated cell sorting; HDAC, histone deacetylase; HAT, histone acetyltransferase; HTS, high throughput screening; NSCLC, nonsmall cell lung cancer; PVDF, polyvinylidendiflouride; rHDAC, recombinant HDAC; SAR, structure−activity relationship; SAHA, suberoylanilide hydroxamic acid; SDS, disodium-dodecylsulfate; SDS-PAGE, SDS polyacrylamide gel electrophoresis; STAT, signal transducers and activators of transcription; TSA, trichostatin A; VPA, valproic acid.

Scheme 2[a]
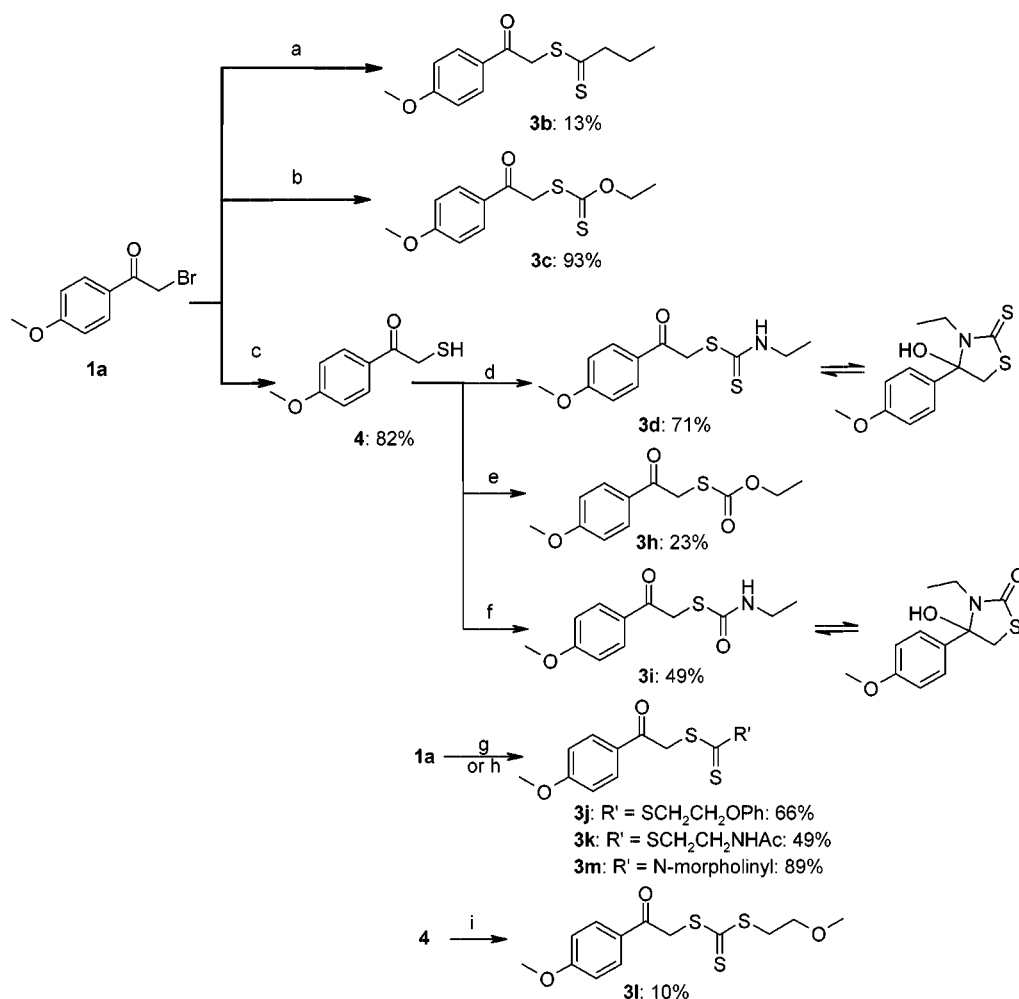
[a] Reagents and conditions: (a) nPrMgCl, CS₂, CuI, THF, −20 °C; (b) EtOH, KOH, CS₂, H₂O, rt; (c) KSAc, THF, 50 °C, then NaOH, MeOH, rt; (d) EtNCS, THF, rt; (e) EtO(C=O)Cl, DIPEA, THF, rt; (f) EtNCO, THF, rt; (g) RC₂H₄SH, NaH, THF, 0 °C, CS₂; (h) morpholine, NaOAc, CS₂, THF, rt; (i) CS₂, NaOH, THF, then EtOC₂H₄Br, rt.

peptide/FK228 (rhomidepsin) and valproic acid (VPA). As shown for SAHA and the natural product trichostatin A (TSA), the hydroxamic acid head group complexes the Zn²⁺ in the active site, thereby inhibiting the enzyme in a substrate competitive manner.[13] So far, HDAC class I isotype selectivity has been shown only for benzamide analogues with MGCD0103 as a prominent example.[14] Selective HDAC6 inhibitors have been rarely described with the hydroxamate analogue Tubacin as one example.[15] Obviously, isotype selective inhibitors will open new avenues for treating cancer and noncancer diseases like rheumatoid arthritis, Crohn's disease or muscle dystrophia, displaying a different overall safety profile.

The structural basis of HDAC inhibition is well established, with the Zn²⁺ complexing head group, a linker/spacer, and the cap group of high structural variability.[13a,16] Nevertheless, the identification of new head groups bearing druglike properties proved to be difficult.[17] Besides the well-studied benzamides and hydroxamates,[18] compounds with a free thiol head group were described as potent and occasionally isotype-selective HDAC inhibitors,[19] but in general cellular activity was very weak.[20] Depsipeptide is a remarkable exception by acting as a prodrug, liberating the reduced sulfhydryl group only intracellular.[21] This concept has also been exploited at similar structures bearing a disulfide moiety derived from thio-pyridine.[22] Different head groups containing sulfur

including thiocarboxylates,[23] thioglycolamides,[24] and α-thio-substituted acetyl compounds[25] have been described. Recently, it was found that a trithiocarbonate group in α-position to the carbonyl moiety represents a promising new head group for HDAC inhibition.[26] In the present study, we report on the exploition of this novel structural motif for HDAC inhibition and its biological activity in detail.

Chemistry. The HDAC inhibitors containing the acetyl trithiocarbonate moiety are typically prepared from an α-halo-acetophenone and conversion with sodium ethyl trithiocarbonate (Scheme 1).[26] The advanced hit compound **2** as well as its methoxy analogue **3a** were obtained in a clean reaction.

Analogues of the trithiocarbonate headgroup were accessible from α-bromo-4-methoxy-acetophenone **1a** in similar conversions, as dithiobutyrate prepared from n-propyl Grignard and carbondisulfide provided access to its dithiocarboxate analogue **3b** (Scheme 2). The corresponding xanthogenate **3c**, the functionalized trithiocarbonates (**3j** and **3k**), and the dithiocarbamate **3m** were prepared from the requisite alcoholate, thiolate, or amine and carbondisulfide followed by addition of the electrophilic bromo-acetophenone. The synthesis of other trithiocarbonate analogues required 2-mercapto-acetophenone **4** as precursor, which was prepared in two steps using potassium thioacetate followed by saponification. The thiol **4** was used to prepare the functionalized

Scheme 3[a]
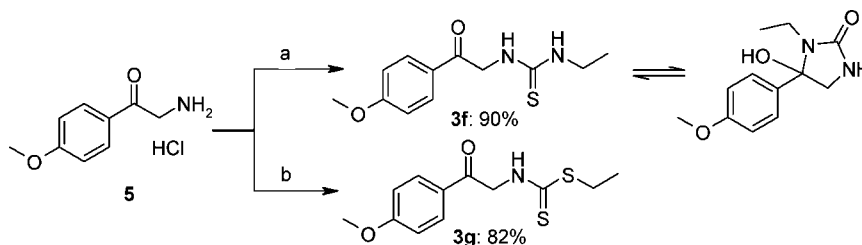
[a] Reagents and conditions: (a) EtNCS, NEt₃, THF, rt; (b) EtBr, CS₂, 1 M NaOH, ethyl acetate/EtOH, rt.

Scheme 4[a]
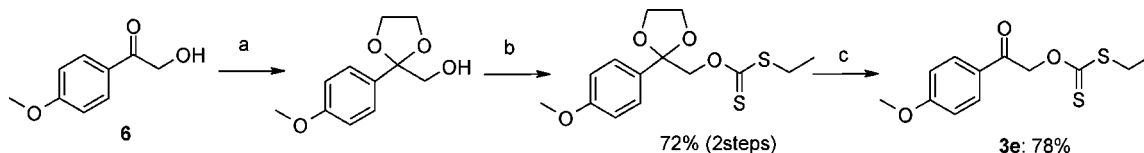
[a] Reagents and conditions: (a) HOC₂H₄OH, amberlyst 15, PhH, 80 °C; (b) NaH, imidazole, THF, 0 °C, then CS₂, then EtI; (c) cat. HCl, THF/H₂O, 60 °C.

Scheme 5[a]

8e: R = 3-AcNH: 70%
8a: R = 4-AcNH: 53%
8f: R = 3-AcNHCH₂: 41%
8g: R = 4-AcNHCH₂: 70%
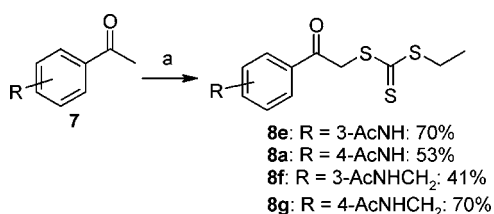
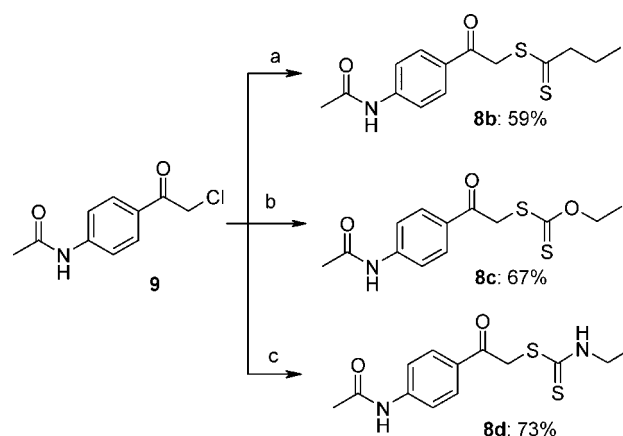[a] Reagents and conditions: (a) PTT, THF, rt; then EtS(C=S)SNa.

trithiocarbonate **3l**, using commercially available methoxy-ethyl bromide (Scheme 2), but the yield for this conversion was found to be rather low. The *O*-ethyl thiocarbonate **3h** and the *N*-ethyl carbamates **3d** and **3i** were prepared in moderate to good yield from **4** by simple addition of ethyl chloroformate, ethyl isothiocyanate, or ethyl isocyanate, respectively.

Scheme 3 illustrates the preparation of nitrogen analogues of the trithiocarbonate moiety. The addition of ethyl isothiocyanate to amino-acetophenone **5** resulted in thiourea **3f**, while conversion with carbondisulfide and ethyl bromide provided the *S*-ethyl carbamate **3g** in high yields. It is noteworthy that all *N*-ethyl derivatives (**3d**, **3i**, and **3f**) exist in an equilibrium with a cyclized species, the ratio being dependent on temperature and solvent environment.

The preparation of the *S*-ethyl dithiocarbonate **3e** proved to be more cumbersome (Scheme 4). 2-Hydroxy-acetophenone **6** was converted into the dioxolane to allow the installation of the required functionality using sodium hydride, carbon sulfide, and ethyl iodide before the protecting group was removed under acid catalysis to yield **3e**.

A one-pot procedure was elaborated to access substituted acetophenone trithiocarbonates, which brominated precursors are not commercially available (Scheme 5).

The acetophenone was brominated in situ with phenyltri-methylammonium tribromide (PTT) in tetrahydrofuran. Decolorization of the orange solution and formation of whitish precipitate indicated the completion of the bromination reaction and a solution sodium ethyl trithiocarbonate solution (stock solution, stored under nitrogen for several weeks) was added to yield **8a** and **8e–g**. Chlorides of type **9** or **10** instead of bromo compounds also represented suitable electrophiles for the preparation of trithiocarbonates (**8h–j**, Scheme 7) as

Scheme 6[a]

8b: 59%

8c: 67%

8d: 73%

[a] Reagents and conditions: (a) i. *n*-PrMgCl, CS₂, CuI, THF, −20 °C, then HCl, H₂O, ii. **9**, NEt₃, DMF, rt; (b) EtOH, KOH, CS₂, H₂O, rt; (c) EtNH₂, aq NaOH, CS₂, DMF, 10 °C to rt.

Scheme 7[a]

8h: R = 4-MeSO₂NH: 64%
8i: R = 4-AcN(Me)CH₂: 83%
8j: R = 4-AcNHCH₂CH₂: 91%
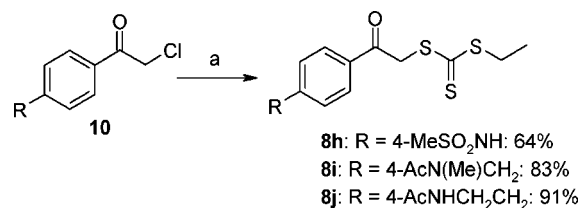
[a] Reagents and conditions: (a) EtS(C=S)SNa, THF, rt.

well as their CH₂-, O-, and NH-analogues (**8b–d**, Scheme 6), which were prepared using similar procedures as described in Scheme 2.

A wide range of trithiocarbonates of type **12** was accessible from substituted acetophenones **7** using the in situ bromination with PTT followed by addition of sodium ethyl trithiocarbonate (Scheme 8, method a and Table 2). This methodolgy was also successful with certain heterocyclic ethanones such as pyrroles (**13**, Scheme 9).

The presence of six-membered nitrogen bearing heterocycles, especially pyridine groups, however, prevented the application of this methodology because no bromide formation with PTT was observed for these substrates. To circumvent this obstacle, alternative bromination methods were examined. NBS bromi-

Scheme 8[a]

12aa–12af & 12al–12av (method a)
12ag (method b)
12ah–12ak (method c)
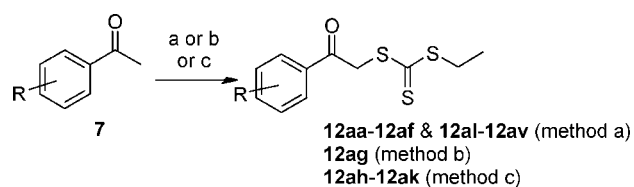
[a] Reagents and conditions: (a) PTT, THF, rt; then EtS(C=S)SNa (method a); (b) TBDMSOTf, NEt$_3$, THF; then NBS, 0 °C, then EtS(C=S)SNa, rt (method b); (c) NaHMDS, THF, −78 °C, then TMSCl, then Br$_2$, then EtS(C=S)SNa, warm to rt (method c).

nation of silylenolethers in situ prepared from the acetophenone and TBDMSOTf followed by addition of sodium ethyl trithiocarbonate was successful for the preparation of **12ag** (Scheme 8, method b, Table 2).

More general applicable was the preparation of silylenolethers using NaHMDS as base and TMSCl in tetrahydrofuran at low temperature. Addition of bromine to the reaction mixture followed by the addition of solution of sodium ethyl trithiocarbonate and warming to rt provided trithiocarbonates bearing pyridine and quinoline substituents (Scheme 8, method c and Table 2). Purification of the resulting products was sometimes difficult and required purification by preparative HPLC.

Several trithiocarbonates containing sulfonamide moieties were prepared from 2-bromo-acetyl-benzenesulfonyl chlorides **14** by subsequent nucleophilic displacement with amines and then sodium ethyl trithiocarbonate (Scheme 10, method d and Table 2).

Outlined in Scheme 11 is the preparation of trithiocarbonate possessing a thiophene core structure. These compounds were derived from 5-acetyl-thiophene-2-carboxylic acid (**15**), which was converted into the amide using *iso*-butyl chloroformiate and *N*-methyl morpholine and subsequent addition of the requisite amine. The reaction mixture was directly treated with PTT followed by addition of sodium ethyl trithiocarbonate, therefore giving access to compounds **16a**–**e** in a four-step one-pot sequence (Table 2).

Its C1-homologues (**18a**–**e**) were prepared in similar sequence from commercially available chloro-acetyl thiophene carboxylic acid **17**, thus the bromination step was omitted in the sequence as shown in Scheme 12 (Table 2).

Finally, two related trithiocarbonates bearing a 2′-pyridinyl-2,5-thieno-acetyl core unit were prepared from commercially available 5-acetyl-2-thienyl-boronic acid (**19**) and respective 2-bromopyridine **20** using Suzuki-coupling conditions to yield the coupling products **21** in acceptable yield (Scheme 13).

The conversion into the trithiocarbonates **22** and **23** required again low temperature α-acetyl deprotonation using sodium hexamethyldisilazide (NaHDMS) followed by silylenolether formation, its subsequent bromination, and finally substitution with sodium ethyl trithiocarbonate.

Biological Results and Discussion. The prepared trithiocarbonates and their analogues were examined for their HDAC inhibiting properties. For this purpose, the compounds were tested using a HDAC isoenzyme mixture purified from HeLa cervical carcinoma nuclei, containing at least HDAC isoenzymes 1, 2, 3, 5, and 8, as well as the recombinant isoforms rHDAC1 and rHDAC6 purified from HEK293 cells.[14] Their cellular activity in HeLa cervical carcinoma cells was evaluated by different assays, namely (i) an enzymatic HDAC activity assay,[27] (ii) by quantification of histone H3 hyperacetylation using a single cell imaging assay,[14] and finally (iii) using the Alamar
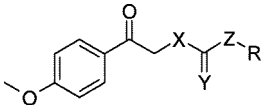
blue proliferation/cytotoxicity assay.[28] Recently, we reported about HDAC inhibitors bearing ethyl trithiocarbonate as a preferred head group[26] found in compounds **2** or **3a**. The lead compound **2** now was more deeply studied for its biochemical properties. Recombinant HDAC isoenzymes were inhibited with IC$_{50}$ = 6.99 μM for rHDAC1 and IC$_{50}$ = 1.25 μM for rHDAC6 (Figure 1B/C). A substrate competitive mode-of-action was demonstrated in enzyme kinetic studies using rHDAC1 with a K_i value of 7 μM calculated from a Lineweaver−Burk plot (Figure 2A). Cellular HDAC activity in HeLa cells was concentration dependently inhibited, evident by an EC$_{50}$ of 4.8 μM for induction of histone H3 hyperacetylation and an IC$_{50}$ of 81.2 μM for inhibition of cellular HDAC activity (Figure 3A/B). A broad cytotoxicity was observed for compound **2** with a mean IC$_{50}$ of 8.31 μM over a panel of 21 different tumor cell lines representing 15 different cancer entities (Figure 5A) and first evidence for a proliferation-dependent cytotoxicity (Figure 5B). Compound **2** induced potent apoptosis in RKO colon carcinoma cells, evident by a massive population of cells in a subG1 cell cycle state (Figure 6A). These experiments with the initial HTS hit compound **2** proved the HDAC inhibitory mode-of-action with similarities to the hydroxamate analogue SAHA in biochemical and cellular assays.

On the basis of the published results for affix variations on ethyl trithiocarbonates,[26] special emphasis was laid on the relevance of the trithiocarbonate moiety itself acting as the HDAC inhibitory head group. For the methoxy trithiocarbonate **3a**, a submicromolar inhibition of the nuclear extract HDAC isoenzyme mixture was determined (IC$_{50}$ = 0.375 μM, Table 1). When the ethyl trithiocarbonate is exchanged for a dithiobutyrate (Z = CH$_2$, **3b**), the HDAC inhibition is slightly enhanced (IC$_{50}$ = 0.123 μM). Similar HDAC inhibition is observed for the dithiocarbamate **3d** (Z = NH, IC$_{50}$ = 0.195 μM), while the dithiocarbonate **3c** is less active (Z = O, IC$_{50}$ = 0.811 μM). Thus, the nuclear extract is inhibited by all four ethyl derivatives **3a**−**3d**.

While the nuclear extract HDACs and rHDAC1 were almost equipotently inhibited by all dithio analogues **3b**−**3d** (1.1−3.4-fold difference, Table 1), the trithiocarbonate **3a** inhibited rHDAC1 about 12-fold less potently (IC$_{50}$ = 4.56 μM) as the nuclear extract. This indicates the presence of another, not tested HDAC isoform(s) or HDAC multiprotein complex distinct to rHDAC1 and present in the nuclear extract, preferentially inhibited by trithiocarbonate representative **3a** compared to other dithio analogues **3b**−**3d**. In contrast, **3a** exhibited a slightly more potent rHDAC6 inhibition (IC$_{50}$ = 1.22 μM), a cytosolic isoenzyme not present in the nuclear extract. About 10 times more potent rHDAC6 inhibition was found for all dithio analogues **3b**−**3d**, especially for dithiocarboxylate **3b** and dithiocarbamate **3d** (Table 1).

For the trithiocarbonate **3a**, its enzymatic inhibition of rHDAC1 correlated well with cellular HDAC inhibition (IC$_{50}$ = 4.67 μM) and is also expressed by inhibition of proliferation/cytotoxicity toward HeLa cells (IC$_{50}$ = 1.96 μM). A direct correlation between rHDAC1 inhibition and cellular activity, however, is not found for dithiocarboxylate **3b** or dithiocarbamate **3d** and is less distinct for the dithiocarbonate **3c**.

The replacement of the phenacyl bound sulfur in the headgroup for oxygen (X = O, **3e**) or nitrogen (X = NH, **3g** or **3f**) results in a complete loss of any HDAC inhibitory activity (Table 1). Finally, substitution of the central sulfur for oxygen was probed for the N- and O-analogues (Y = O, **3h** and **3i**). These compounds exhibited HDAC inhibition in a similar range as the corresponding sulfur analogues (Y = S, **3c** and **3d**) for

Table 1. Enzymatic and Cellular Assay Results for Compounds **3**[a]

| compd	X	Y	Z	R	HDAC nuc IC$_{50}$ [μM]	rHDAC1 IC$_{50}$ [μM]	rHDAC6 IC$_{50}$ [μM]	cell HDAC IC$_{50}$ [μM]	HeLa cytotoxicity IC$_{50}$ [μM]
3a	S	S	S	C$_2$H$_5$	0.375	4.56	1.22	4.67	1.96
3b	S	S	CH$_2$	C$_2$H$_5$	0.123	0.422	0.110	3.41	5.71
3c	S	S	O	C$_2$H$_5$	0.811	1.38	0.448	4.72	4.64
3d	S	S	NH	C$_2$H$_5$	0.195	0.215	0.094	nd	7.80
3e	O	S	S	C$_2$H$_5$	16% @ 32 μM	6% @ 32 μM	16% @ 32 μM	28% @ 50 μM	2.99
3f	NH	S	NH	C$_2$H$_5$	−6% @ 30 μM	nd	nd	nd	5.81
3g	NH	S	S	C$_2$H$_5$	−3% @ 32 μM	−17% @ 32 μM	−8% @ 32 μM	nd	26% @ 50 μM
3 h	S	O	O	C$_2$H$_5$	2.81	21.2	5.36	9.79	18.5
3i	S	O	NH	C$_2$H$_5$	0.115	0.368	0.132	3.18	13.3
3j	S	S	S	C$_2$H$_4$OPh	0.128	9.72	4.57	11.6	5.46
3k	S	S	S	C$_2$H$_4$NHAc	0.467	7.51	1.64	3.47	11.1
3l	S	S	S	C$_2$H$_4$OCH$_3$	0.293	8.94	2.13	5.53	7.88
3m	S	S	bond	−*N*-morpholinyl	2% @ 32 μM	0% @ 32 μM	−2% @ 32 μM	0% @ 32 μM	−8% @ 50 μM

[a] Biochemical and cellular assays were done in replicate and mean values are shown. IC$_{50}$ values were calculated from respective concentration−effect curves. Inhibition of cellular HDAC enzymatic activity and cytotoxicity was quantified in HeLa cervical carcinoma cells. nd: not determined.
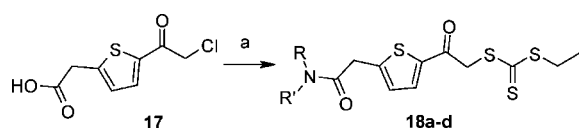
Scheme 9[a]

13: 98%
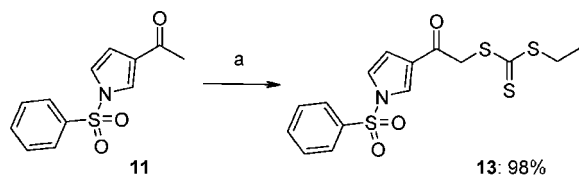
[a] Reagents and conditions: (a) PTT, THF, rt; then EtS(C=S)SNa.

Scheme 10[a]

12aw-12az
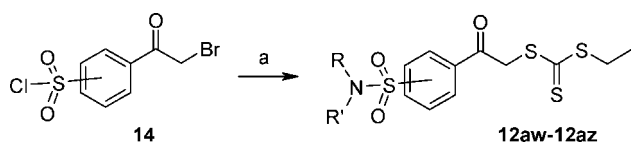
[a] Reagents and conditions: (a) RR'NH, DIPEA, THF, rt; then EtS(C=S)SNa (method d).

Scheme 11[a]

16a-e
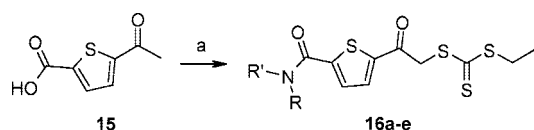
[a] Reagents and conditions: (a) NMM, IBCF, THF, 0 °C, then RR'NH, rt, then PTT, then EtS(C=S)SNa. NMM: *N*-methyl-morpholine; IBCF: *i*-butylchloroformiate.

Scheme 12[a]

18a-d

[a] Reagents and conditions: (a) NMM, IBCF, THF, 0 °C, then RR'NH, rt, then EtS(C=S)SNa. NMM: *N*-methyl-morpholine; IBCF: *i*-butylchloroformiate.

the isoenzyme mixture, rHDAC1, and rHDAC6 (Table 1). The cellular HDAC inhibition and cytotoxicity of derivatives **3h** and **3i** was about 2-fold weaker compared to the sulfur analogues, resulting in a less pronounced correlation between rHDAC1 inhibition and cellular HDAC activity.

In a next step, substitution of the ethyl group of the trithiocarbonates were investigated with the option to improve physicochemical properties of such compounds. Introduction of phenoxy- (**3j**) and methoxy-groups (**3l**) were tolerated as the nuclear extract (IC$_{50}$ = 0.128 and 0.293 μM, respectively, Table 1) was inhibited in a similar range as the unsubstituted ethyl derivative **3a** (IC$_{50}$ = 0.375 μM). Similarly, the *N*-acetamide substitutent (**3k**) was found to be an active HDAC inhibitor. All three substituted ethyl derivatives **3j**−**3l** showed slightly decreased rHDAC1 and rHDAC6 activity compared to **3a**. The inhibition of cellular HDAC activity was found to be similar to **3a** and correlating well with rHDAC1 inhibition (Table 1). Interestingly, the most sterically demanding phenoxy derivative **3j** showed the lowest activity in both test systems. In contrast to cellular HDAC inhibitory activity, the cytotoxicity of the substituted derivatives **3j**−**3l** is significantly weaker compared to their unsubstituted parent compound **3a**. While variations of the ethyl moiety of trithiocarbonates were compatible with HDAC inhibition, a variation of dithiocarbamates toward more bulky, secondary dithiocarbamates lead to completely inactive compounds (**3m**).

These results for the variation of the head group were reconfirmed in the structurally related *N*-acetamide series **8a**−**8d** (Table 2). Again, all four analogues inhibit the nuclear extract in a similar range (IC$_{50}$ values from 87 to 386 nM, Table 2) but more potently than the methoxy compounds **3a**−**3d**. Again, the differences for the nontrithiocarbonates **8b**−**8d** between inhibition of nuclear extract and rHDAC1 are subtle (1.4−1.9 times), while **8a** inhibits rHDAC1 about 5 times less potently. Potent rHDAC6 inhibition is found for all *N*-acetamide analogues **8a**−**8d**, especially dithiocarboxylate **8b** and dithiocarbamate **8d**, showing low nanomolar inhibition (IC$_{50}$ = 23 and 18 nM, respectively, Table 2).

The complete inhibition of nuclear extract HDACs, rHDAC1, and rHDAC6 is exemplified for **8b** in Figure 1. As seen before, a good correlation between enzymatic and cellular activity is found only for the trithiocarbonate **8a**, whereas for the dithio analogues **8b**−**8d**, this correlation is less distinct (Table 2). Respective concentration−effect curves for cellular HDAC inhibition and histone H3 hyperacetylation exemplified for **8c** are shown in Figure 3 (IC$_{50}$ values of 2.9 and 28 μM, respectively), verified by Western

Scheme 13[a]
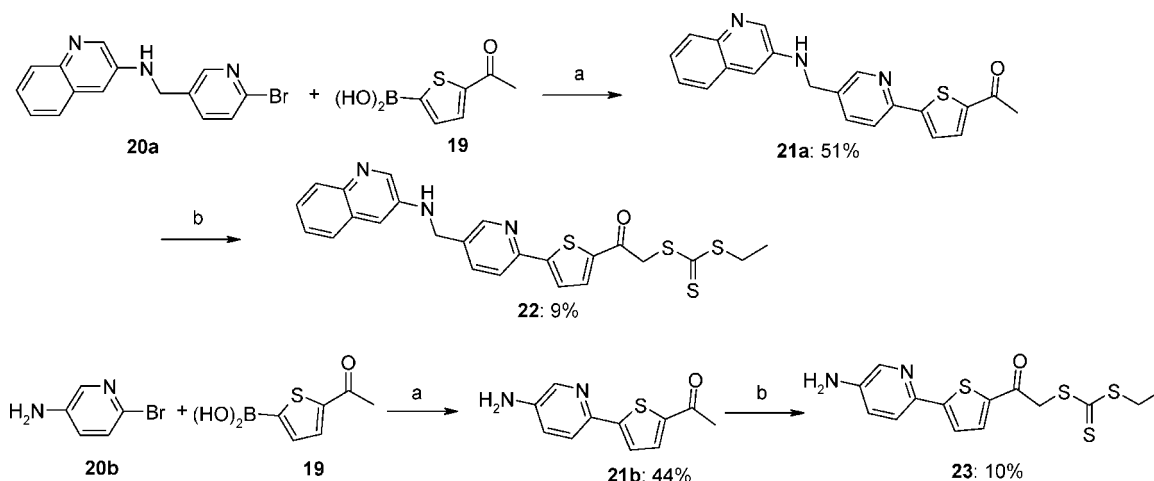
[a] Reagents and conditions: (a) Pd(dppf)Cl$_2$, Cs$_2$CO$_3$, dioxane/H$_2$O, rt; (b) NaHMDS, THF, −78 °C, then TMSCl, then Br$_2$, then EtS(C=S)SNa, warm to rt; NaHMDS: sodium hexamethyldisilazide.
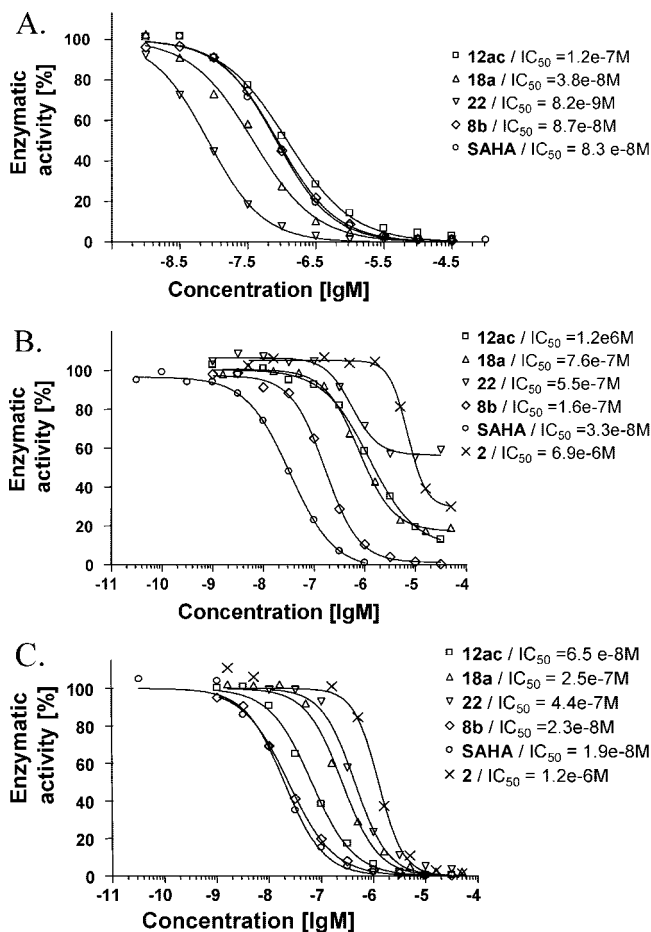

Figure 1. Inhibition of HDAC enzymatic activity. Trithiocarbonate analogues, namely **2** as initial HTS hit, **3b** (dithiobutyrate analogue), **12ac** (phenylamide analogue), **18a** and **22** (thiophene analogues) were tested for inhibition of HeLa nuclear extract HDAC activity (A), rHDAC1 (B), and rHDAC6 (C) as class I and IIb representatives, respectively. SAHA was included as a reference HDAC inhibitor with the hydroxamate head group. IC$_{50}$ values calculated from the concentration−effect curves using Graphpad prism nonlinear curve fitting are shown.

blotting for histone H3 hyperacetylation and p21$^{\text{waf}}$ induction in Figure 4 for **8b** and **8c**.

Having identified an amide substitutent at the phenacyl moiety to be beneficial for HDAC inhibition, several small analogues of **8a** were tested. Introduction of the *N*-acetyl substituent in *meta*-position (**8e**) instead of *para*-position (**8a**) lead to a decrease in enzymatic (about 2-fold) and cellular (about 5-fold) activity. Even more prominent was this difference between the *meta*- and *para*-position in the case of C1-homologues (**8f** and **8g**). While *para*-analogue **8g** exhibited slightly reduced HDAC activity compared to **8a** (about 2−4 times, Table 2), the *meta*-derivative **8f** was more than 10-fold less active in nuclear extract and rHDAC1 inhibition (IC$_{50}$ values of 6.59 and 38.2 μM, respectively). Interestingly, rHDAC6 inhibition by **8f** and the cellular HDAC inhibition were found to be less reduced (about 2−3 times). Other *para*-*N*-acetyl derivatives were also studied. The *N*-methylsulfonamide **8h** proved to be a weaker HDAC inhibitor in the overall profile. *N*-acetyl-methylation of the C1-homologue (**8i**) or C2-homologenation (**8j**) resulted in potent rHDAC1 inhibitors in submicromolar range (IC$_{50}$ values of 0.946 and 0.607 μM, respectively, Table 2), but their cellular activity, especially cytotoxicity toward Hela cells, were surprisingly modest.

Next, trithiocarbonates with a phenylacetyl moiety as the core bearing larger amide substituents were studied in detail for their HDAC inhibitory effects (Table 3). Simple phenyl amide derivatives **12aa**−**12ad** proved to be effective HDAC inhibitors in regard to the HDAC isoenzyme mixture displaying submicromolar activity. In general, those compounds possess a remarkable selectivity for rHDAC6 over rHDAC1. The complete inhibition of nuclear extract, rHDAC1, and rHDAC6 is shown for **12ac** in Figure 1. A substrate competitive mode-of-action for inhibition of rHDAC6 was determined with a K_i value of 0.11 μM (Figure 2B). In A549 NSCLC cells, α-tubulin hyperacetylation as a hallmark for cellular HDAC6 inhibition was strongly induced by **12ac** at 10 μM concentration, whereas the effect on histone H3 hyperacetylation was weak (Figure 4B). This nicely proved the HDAC6 selectivity also in a cellular context.

The differences in activity between acetyl benzoic acid derived anilides **12aa** and **12ab** and the inverse amides **12ac** and **12ad** are marginal except for rHDAC6 inhibition, which was more effectively inhibited by **12ac** and **12ad**. As seen before for small amides, the position of ring substitution has a strong influence on rHDAC1 inhibition: *meta*-substituted derivatives **12aa** and **12ac** inhibit rHDAC1 with low micro-
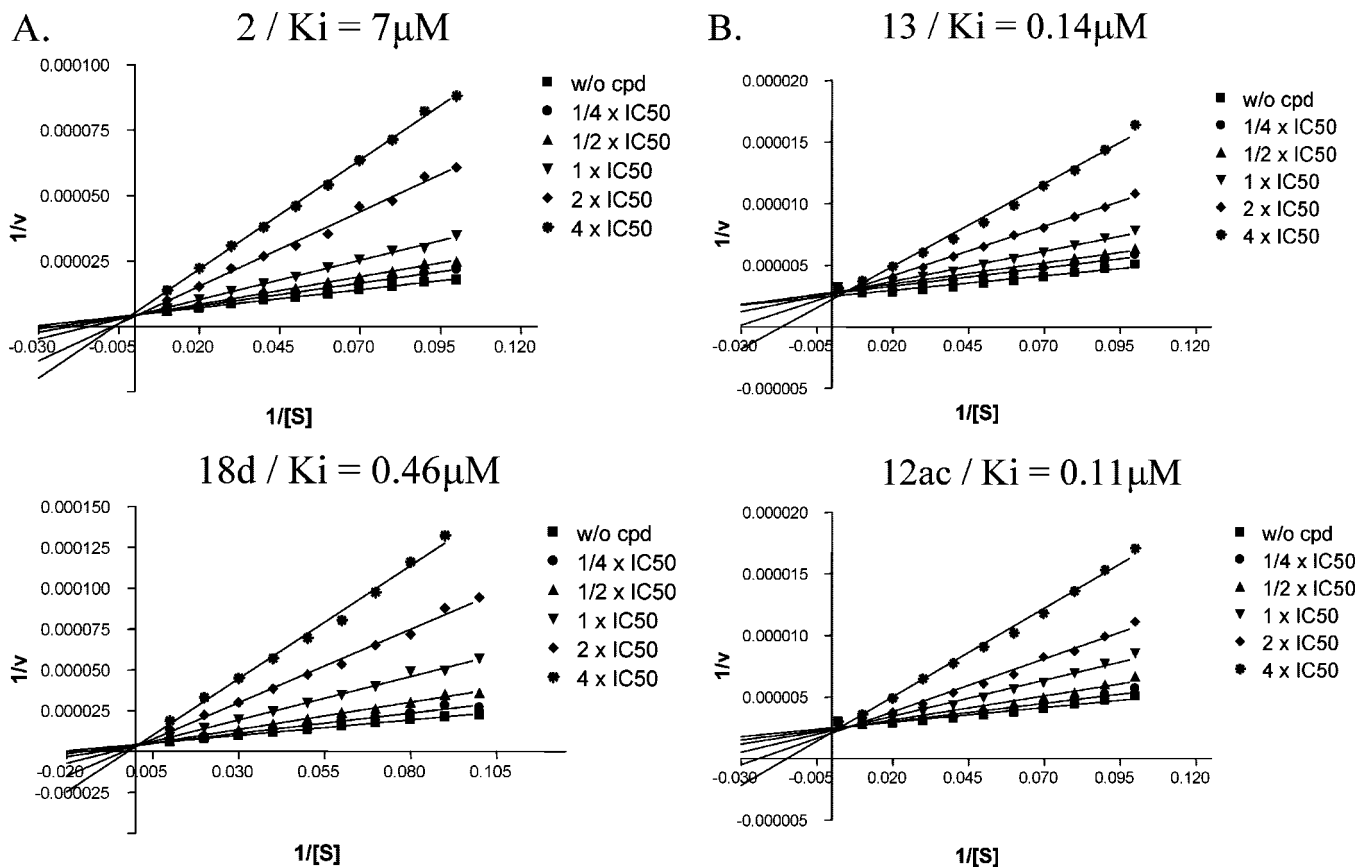
Figure 2. Enzyme kinetic analysis of rHDAC1 and rHDAC6 inhibition. The initial hit **2** and the thiophene analogue **18d** were tested for inhibition of rHDAC1 enzymatic activity at various substrate concentrations up to 100 μM. Respective Lineweaver–Burk plots with calculated K_i values are shown in (A). A similar analysis was done for isoenzyme selective analogues **12ac** and **13** regarding inhibition of rHDAC6 at various substrate concentrations up to 100 μM. Respective Lineweaver–Burk plots with calculated K_i values are shown in (B). Ac-GGK(Ac)-AMC was used as the substrate for both, rHDAC1 and rHDAC6 assays.
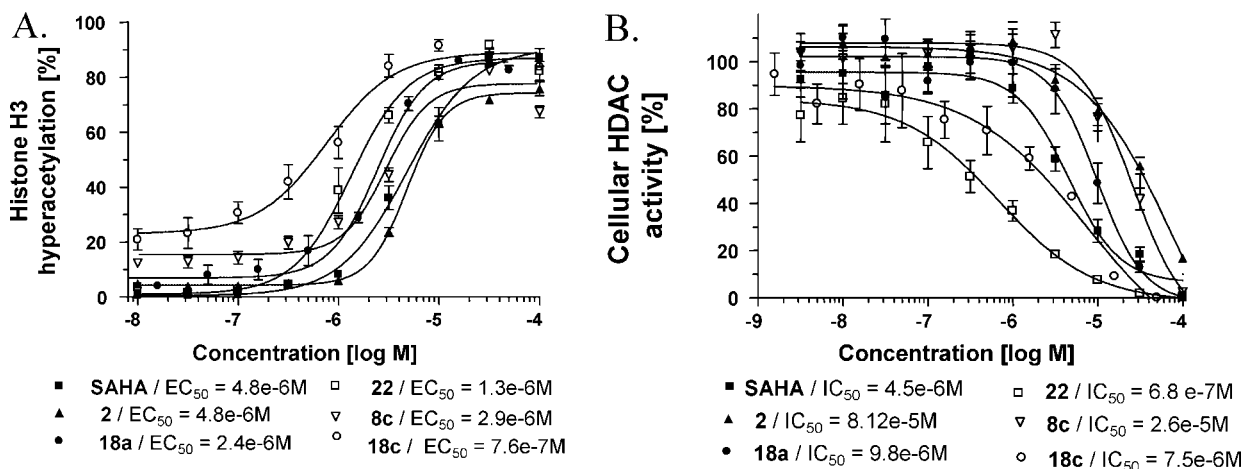

Figure 3. Inhibition of HDAC activity in HeLa cells. The inhibition of cellular HDAC activity by selected analogues **2**, **8c**, **18a**, **18c**, **22**, and SAHA as reference was measured in two independent assays in HeLa cells. The induction of histone H3 hyperacetylation was quantified by single-cell image analysis using the Cellomics Array Scan (A). The inhibition of HDAC enzymatic activity was quantified with the cell permeable HDAC substrate Boc-K(Ac)-AMC. After cell lysis, only the deacetylated substrate Boc-K-AMC is cleaved by trypsin with subsequent release of the fluorophore AMC.

molar activity (IC_{50} values of 1.67 and 1.22 μM, respectively). The corresponding *para*-substituted derivatives, however, strongly loose their rHDAC1 inhibitory activity in case of the aniline derivative **12ad** (IC_{50} = 10.4 μM) or almost completely in case of benzoic acid derivative **12ab** (IC_{50} = 27.9 μM). Structural rigidity of the phenyl amide moiety might be an explanation for this remarkable isoenzyme selectivity, as the corresponding structurally more

flexible *para*- and *meta*-substituted sulfonamide derivates **12ae** and **12af** do not discriminate in their rHDAC1 activity. The conformationally restricted amino-quinazoline **12ag** also inhibited the HDAC nuclear extract and rHDAC6 in submicromolar concentration, but rHDAC1 inhibition is also significantly reduced (IC_{50} = 25.8 μM). The amides of 3-pyridine-carboxylic acid and 3-quinoline-carboxylic acid, **12ah**−**12ak**, were found to be strong HDAC inhibitors (IC_{50}
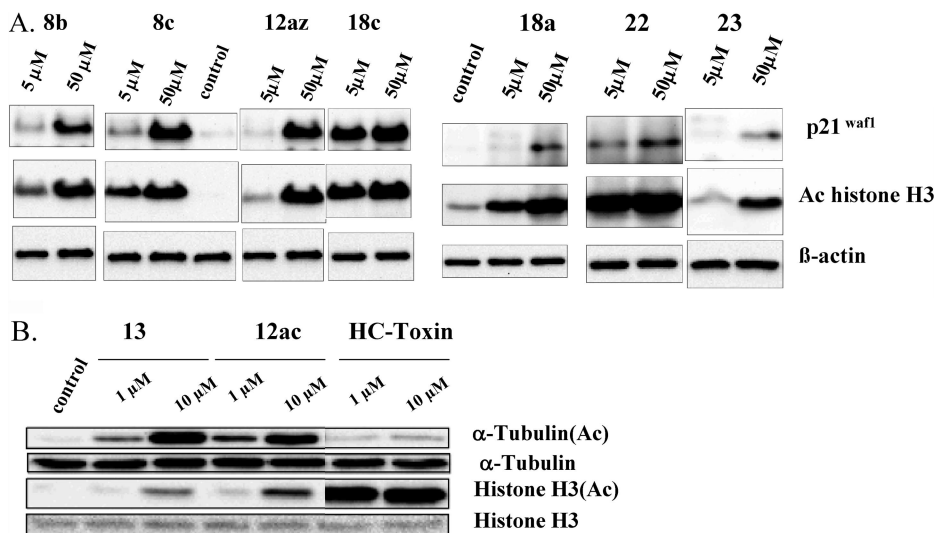
Figure 4. Induction of p21^{waf} expression, histone H3, and α-tubulin hyperacetylation. The induction of histone H3 K$^{1-20}$ hyperacetylation and p21^{waf1} as a HDAC inhibitor marker gene was analyzed in HeLa cells, treated with analogues **8b**, **8c**, **12az**, **18a**, **18c**, **22**, and **23** at concentrations of 5 and 50 μM for 24 h (A). As a control, rehybridization was done with a β-actin specific antibody. The induction of histone H3 K$^{1-20}$ and α-tubulin hyperacetylation was studied in A549 NSCLC cells treated for 24 h with the HDAC6 selective analogues **12ac** and **13** (B). The natural product HC-toxin was included as HDAC inhibitor with weak, μM inhibition of HDAC6. As a control, rehybridization was done with antibodies specific for histone H3 or α-tubulin.
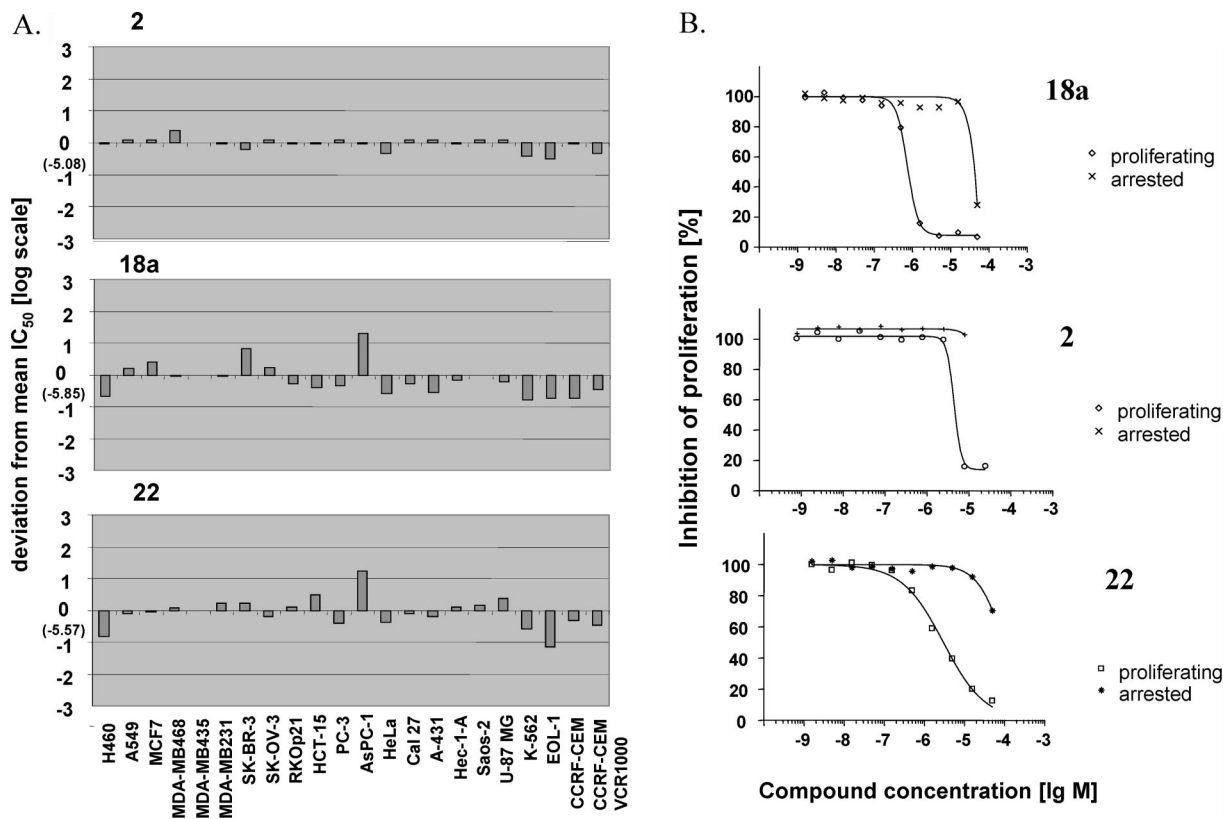

Figure 5. Cytotoxicity profile for selected trithiocarbonate analogues. The overall cytotoxicity profile was studied for **2** as the initial HTS hit and the potent thiophene analogues **18a** and **22**. A selection of 21 different solid and hematological tumor cell lines representing 15 different histotypes was treated for 72 h with the HDAC inhibitors before quantification of metabolic activity, correlating with cell viability/cell number. Mean graph blots with the deviation from the mean IC$_{50}$ expressed in log IC$_{50}$ [M] are shown in (A). In this graphic representation, the mean IC$_{50}$ value for a given compound is defined as "0" and deviations of individual IC$_{50}$ values (log IC$_{50}$ [M]) to higher and lower potency are expressed as negative and positive values, respectively. Mean IC$_{50}$ values were determined as 8.31 μM (-5.08) for **2**, 1.41 μM (-5.85) for **18a**, and 2.37 μM (-5.57) for **22**. Individual concentration$-$effect curves are shown for proliferating and arrested, nonproliferating RKO p21^{waf1} colon carcinoma cells in (B). RKO p21^{waf1} cells were arrested by induction of the cdk inhibitory p21^{waf1} protein.

as low as 36 nM) and preferential inhibition of rHDAC6. rHDAC6 selectivity, however, is less prominent for the *para*-substituted derivatives **12ai** and **12ak**, as their rHDAC1 inhibition is in the micromolar range. For these compounds,

the rHDAC1 inhibition correlates well with cellular HDAC inhibition resulting in submicromolar cellular activity, albeit their cytotoxic activity is weak. More evidence for the dependence of rHDAC1 inhibition on structural flexibility

Table 2. Enzymatic and Cellular Assay Results for Compounds **8**[a]

compd	X	R	HDAC nuc IC$_{50}$ [μM]	HDAC1 IC$_{50}$ [μM]	rHDAC6 IC$_{50}$ [μM]	cell HDAC IC$_{50}$ [μM]	HeLa cytotoxicity IC$_{50}$ [μM]
8a	S	4-AcNH	0.318	1.68	0.180	0.857	1.46
8b	CH$_2$	4-AcNH	0.087	0.164	0.023	1.37	6.41
8c	O	4-AcNH	0.386	0.536	0.090	26.2	3.61
8d	NH	4-AcNH	0.094	0.141	0.018	1.12	11.0
8e	S	3-AcNH	0.506	2.93	0.329	3.28	9.38
8f	S	3-AcNHCH$_2$	6.59	38.24	0.816	6.82	11.3
8g	S	4-AcNHCH$_2$	0.719	7.12	0.346	2.07	17.9
8h	S	4-MeSO$_2$NH	1.26	6.11	1.09	8.95	45.8
8i	S	4-AcN(Me)CH$_2$	0.384	0.946	0.256	6.33	21.5
8j	S	4-AcNHCH$_2$CH$_2$	0.587	0.607	0.102	1.48	12.8

[a] Biochemical and cellular assays were done in replicate and mean values are shown. IC$_{50}$ values were calculated from respective concentration−effect curves. Inhibition of cellular HDAC enzymatic activity and cytotoxicity was quantified in HeLa cervical carcinoma cells.
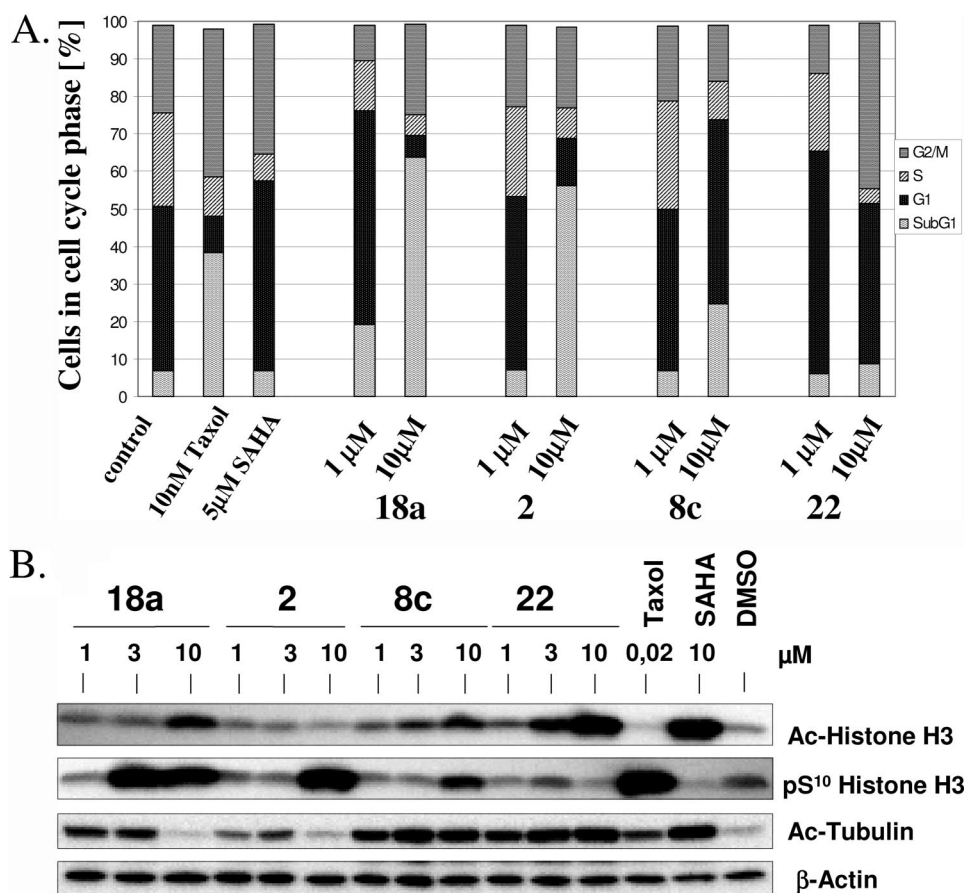

Figure 6. Cell cycle analysis and induction of histone H3S^{10} phosphorylation. The effects of selected analogues **2**, **8c**, **18a**, and **22** on the cell division cycle of RKO colon carcinoma cells was studied by flow cytometry. RKO cells were treated for 24 h with the trithiocarbonate analogues at 1 and 10 μM concentration. The percentage of cells in apoptosis (subG1), G1(2N), S, and G2/M (4N) was determined and is shown in a column diagram in (A). 10 nM taxol as a tubulin interacting, antimitotic agent and 5 μM SAHA were included as control agents. The phosphorylation of histone H3 at residue S^{10} in RKO cells treated for 24 h with **2**, **8c**, **18a**, and **22** at 1, 3, and 10 μM concentration was analyzed by Western blotting (B). Hyperacetylation of histone H3 K$^{1-20}$ as well as α-tubulin was analyzed in parallel. As a control, rehybridization was done with a β-actin specific antibody.

of the core phenyl substitution is provided by compounds **12al**−**12an**. A more than 8-fold difference in rHDAC1 inhibition between *meta*- and *para*-substituted benzylamides **12al** and **12am** was observed, but the constitutional *para*-isomer **12an**, which possess a less rigid connection to the phenyl core, again retained rHDAC1 inhibition (IC$_{50}$ = 0.523 μM). Another pair of *meta*- and *para*-substituted phenyl with potent HDAC inhibitory properties are phenoxy-ethylamino carboxamides **12ao** and **12ap**, which are low submicromolar HDAC inhibitors in the enzymatic assays as well as potent
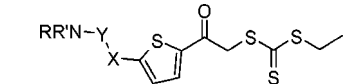
inhibitors of cellular HDAC activity, but again weakly cytotoxic. A final example for the loss of rHDAC1 inhibitory efficacy by the structural rigidity of *para*-substituted phenyl analogues represents the bis-phenyl urea **12aq**, which is 30-fold more active toward rHDAC6 (IC$_{50}$ = 0.606 μM) and 470-fold more active toward the nuclear extract isoenzyme mixture (IC$_{50}$ = 0.040 μM) compared to rHDAC1 (IC$_{50}$ = 18.8 μM).
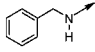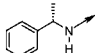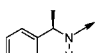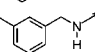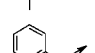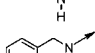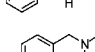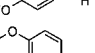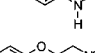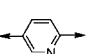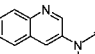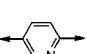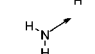
The next series of trithiocarbonates that were probed for HDAC inhibition were phenylsulfonamides (Table 3). Four

Table 3. Enzymatic and Cellular Assay Results for Compounds **12**[a]
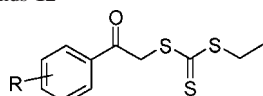
Cpd	Position of R	R	Method of Preparation	Yield [%]	HDAC nuc IC$_{50}$ [µM]	rHDAC1 IC$_{50}$ [µM]	rHDAC6 IC$_{50}$ [µM]	cell HDAC IC$_{50}$ [µM]	HeLa cytotox IC$_{50}$ [µM]
12aa	3-		a	18	0.124	1.67	0.517	1.23	2.40
12ab	4-		a	30	0.074	27.9	0.521	1.11	25.8
12ac	3-		a	8	0.120	1.22	0.065	0.964	8.23
12ad	4-		a	30	0.074	10.4	0.175	7.46	15.8
12ae	3-		a	28	0.127	1.55	0.104	2.78	11.9
12af	4-		a	25	0.042	1.87	0.382	0.800	9.04
12ag	4-		b	27	0.379	25.8	0.390	2.99	2.645
12ah	3-		c	12	0.184	0.388	0.030	0.646	7.02
12ai	4-		c	7	0.174	1.16	0.421	0.865	5.16
12aj	3-		c	6	0.036	0.592	0.089	0.483	9.61
12ak	4-		c	11	0.066	0.980	0.119	0.748	50.0
12al	3-		a	63	0.049	0.672	0.195	0.533	13.1
12am	4-		a	49	0.090	5.78	0.830	1.50	23.9
12an	4-		a	5	0.046	0.523	0.301	0.632	12.7
12ao	3-		a	45	0.027	0.328	0.198	0.500	10.2
12ap	4-		a	53	0.032	0.712	0.483	0.964	18.2
12aq	4-		a	50	0.040	18.8	0.606	1.19	20.2
12ar	4-		a	9	0.079	1% @ 30 µM	1.450	nd	0% @ 50 µM
12as	4-		a	69	0.008	0.589	0.340	0.299	6.08
12at	4-		a	68	0.025	2.49	0.979	1.74	10.4
12au	3-		a	28	0.048	3.46	1.25	9.08	46.6
12av	4-		a	68	0.016	0.227	0.245	0.377	4.32
12aw	3-		d	35	0.015	0.530	0.519	2.77	5.17
12ax	3-		d	4	0.110	5.33	2.04	nd	43% @ 50 µM
12ay	3-		d	13	0.097	1.56	0.181	1.15	7.74
12az	3-		d	32	0.014	0.501	0.431	1.86	9.18

[a] Biochemical and cellular assays were done in replicate and mean values are shown. IC50 values were calculated from respective concentration−effect curves. Inhibition of cellular HDAC enzymatic activity and cytotoxicity was quantified in HeLa cervical carcinoma cells.

Table 4. Enzymatic and Cellular Assay Results for Compounds **16** and **18**[d]

Cpd	X	Y	Amine NRR'	Yield [%]	HDAC nuc IC$_{50}$ [μM]	rHDAC1 IC$_{50}$[μM]	rHDAC6 IC$_{50}$ [μM]	cell HDAC IC$_{50}$ [μM]	HeLa cytotox IC$_{50}$[μM]
16a	bond	CO		12[a]	0.019	0.340	0.044	0.411	13.0
16b	bond	CO		6[a]	0.049	0.497	0.135	1.03	15.8
16c	bond	CO		44[a]	0.044	0.725	0.165	1.45	15.8
16d	bond	CO		21[a]	0.015	0.587	0.396	0.836	31.3
16e	bond	CO		22[a]	0.063	31.6	0.245	0.423	50.0
18a	CH$_2$	CO		13[b]	0.038	0.762	0.250	9.84	0.710
18b	CH$_2$	CO		15[b]	0.026	0.887	0.175	0.600	1.45
18c	CH$_2$	CO		3[b]	0.010	0.251	0.116	7.53	6.61
18d	CH$_2$	CO		17[b]	0.018	0.385	0.204	0.624	5.78
22		CH$_2$		9[c]	0.008	0.555	0.438	0.683	2.70
23		bond		10[c]	0.083	0.831	0.043	1.18	0.452

[a] Preparation according to Scheme 11. [b] Preparation according to Scheme 12. [c] Preparation according to Scheme 13. [d] Biochemical and cellular assays were done in replicate and mean values are shown. IC50 values were calculated from respective concentration-effect curves. Inhibition of cellular HDAC enzymatic activity and cytotoxicity was quantified in HeLA cervical carcinoma cells.

4-chloro-phenyl derivatives were compared and, as expected, the *para*-4-chloro-aniline carboxamide **12ar** was inactive in the rHDAC1 enzyme assay, while the corresponding sulfonamide **12as** exhibited submicromolar rHDAC1 and cellular HDAC inhibiton, besides a very potent inhibition of nuclear HDACs (IC$_{50}$ = 8 nM). The constitutional analogue **12at** was considerably less potent toward rHDAC1 (IC$_{50}$ = 2.49 μM), and the *meta*-substituted analogue **12au** has even lower enzymatic inhibitory activity that is also reflected in low cellular HDAC inhibition. The biochemical discrimination between *meta*- and *para*-substituted benzene sulfonamides was probed for the 4-methoxy-aniline sulfonamides **12av** and **12aw**. Both isomers were found to be potent inhibitors of the nuclear extract, but in contrast to the carboxamides (e.g., **12aa** and **12ab**), the *para*-substituted sulfonamide showed slightly enhanced activity at rHDAC1 and rHDAC6 (about 2-fold) and clearly superior cellular HDAC inhibition. Interestingly, all activity was 10-fold reduced by methylation of the sulfonamide moiety (**12ax**). Several other amino-aryl sulfonamides were low submicromolar HDAC inhibitors with cytotoxic activity of IC$_{50}$ = 7.7 and 9.18 μM for **12ay**−**12az**, respectively. The cellular activity of **12az** as HDAC inhibitor was proven by a strong induction of p21^{waf1} and histone H3 hyperacetylation at 50 μM concentration in HeLa cells (Figure 4A).

The HDAC inhibitory activity of the structurally related pyrrole-*N*-sulfonamide **13** was also studied in more detail (Scheme 9). Nuclear HDACs were very potently inhibited with an IC$_{50}$ of 9 nM, while rHDAC1 inhibition was about 200-fold weaker (IC$_{50}$ = 2.1 μM). Compound **13** was found to be a very potent and selective HDAC6 inhibitor in biochemical (IC$_{50}$ = 56 nM) and cellular (EC$_{50}$ ≈ 5 μM) assays (Figure 4B), displaying a substrate competitive mode-of-action as determined by Lineweaver−Burk enzyme kinetic analysis (K_i = 0.14 μM, Figure 2B).

Trithiocarbonates bearing a 2,5-disubstituted thiophene core instead of benzene as in compounds of type **16** were also potent HDAC inhibitors (Table 4). The HDAC isoenzyme mixture was inhibited with IC$_{50}$ values from 19 to 63 nM, while the inhibition of rHDAC6 was weaker, especially for the sterically more demanding 3,5-dimethylbenzyl amine derivative **16d**. Remarkably, rHDAC1 was inhibited by all benzyl amine derivatives **16a**−**16d** with IC$_{50}$ values between 0.34 and 0.73 μM (Table 4), but as seen for the phenyl compounds **12**, the rigidified aniline amide **16e** was almost inactive (IC$_{50}$ = 31.6 μM). Noteworthy, the two enantiomers **16b** and **16c** had almost identical inhibitory activity. The activity of the amides **16** in biochemical assays was reflected in potent cellular enzymatic HDAC inhibition (IC$_{50}$ values from 0.41 to 1.45 μM), but very weak cytotoxicity was determined.

If the structural rigidity in the thienyl carboxamide bond was reduced by introduction of a methylene linker as in aryl-bearing amides **18a**−**18d**, potent HDAC inhibitors were obtained. For all derivatives, also reasonable rHDAC1 inhibitory activity was found, even for aniline derived carboxamides as **18c** (IC$_{50}$ = 0.25 μM, Table 4), which was more active as its benzylamine analogue **18b** (IC$_{50}$ = 0.89 μM). rHDAC6 inhibition was also observed for **18a**−**18d**. Complete inhibition of nuclear extract, rHDAC1, and rHDAC6 isoenzymes is shown for **18a** in Figure

1, and the substrate competitive mode-of-action for **18d** was proven for **18d** exemplarily (K_i = 0.46 μM, Figure 2A). Compound **18a** displays potent cytotoxicity toward HeLa cells (IC$_{50}$ = 0.71 μM) and was studied together with the close analogue **18c** in more detail. Histone H3 hyperacetylation is induced by **18a** and **18c** with EC$_{50}$ values of 2.4 and 0.76 μM, respectively (Figure 3A), also seen in respective Western Blot experiments for p21^{waf1} and acetylated histone H3 (Figure 4A). Inhibition of cellular HDAC enzymatic activity was up to 10-fold weaker for both analogues. Compound **18a** was also characterized using the 21 tumor cell line panel, depicting a mean cytotoxicity of IC$_{50}$ = 1.41 μM, quite comparable to SAHA (mean IC$_{50}$ = 3.3 μM)[29] with some preferential activity toward hematological tumors (Figure 5).

Finally, the two pyridinyl-thienoacetyl derivatives **22** and **23** were studied. Both compounds exhibited potent HDAC inhibition in the enzymatic assays. While the amino-quinoline substituted derivative **22** was a very potent inhibitor of the nuclear extract (IC$_{50}$ = 8 nM, Table 4), inhibition of rHDAC1 and rHDAC6 with IC$_{50}$ values of 0.56 and 0.44 μM, respectively, was significantly weaker. The concentration-dependent activity of derivative **22** in the biochemical HDAC assays is shown in Figure 1, with a partial inhibition of rHDAC6 only. The 5-amino-pyridinyl bearing trithiocarbonate **23** was also active in the HeLa nuclear extract and rHDAC1 assays but with diminished potency. Nevertheless, rHDAC6 was potently inhibited with IC$_{50}$ = 43 nM. For both compounds, the activity in the cellular HDAC activity assay and cytotoxicity were in the same range. Respective cellular data for histone H3 hyperacetylation, p21^{waf1} induction, and HDAC enzymatic activity are shown for analogues **22** and **23** in Figure 3A/B and Figure 4A. Compound **22** was characterized using the 21 tumor cell line panel, depicting a mean cytotoxicity of IC$_{50}$ = 2.37 μM and a selectivity pattern similar to **18a** (Figure 5).

HDAC inhibitors are well-known for affecting cell cycle regulation, depleting cells in the S-phase while transiently arresting in G1 and G2/M as shown for 5 μM SAHA treated RKO colon carcinoma cells in Figure 6. For most cytotoxic trithiocarbonate analogues, a partial proliferation-dependent cytotoxicity was seen in the RKO p21^{waf1} cell system, high-lighted for compounds **18a** and **22** in Figure 5B. This was unexpected, although a partial proliferation-dependent cytotoxicity was seen for selected benzamide analogues in previous studies as well (data not shown). We therefore investigated the effects on RKO cell cycle distribution by compounds **2**, **8c**, **18a**, and **22** in more detail. All analogues induced depletion of S-phase cells and apoptosis after 24 h at 10 μM concentration (Figure 6A). At 1 μM concentration, a partial arrest in G1 is evident for the thiophene analogues **18a** and **22**, a partial arrest in G2/M seen for **22** at the higher concentration of 10 μM. Recently, the interaction of HDAC3 with the mitotic kinase Aurora B and a HDAC3 dependent phosphorylation of histone H3 at residue S^{10} by Aurora B was shown.[30] In this study, hydroxamate analogues induced a strong reduction of histone H3 S^{10} phosphorylation, a marker for mitotic arrest. This has been explained by dissociation of inactive HDAC3 from the Aurora B complex and subsequent hyperacetylation of histone H3 at residue K^9.[30] We therefore investigated the effect of selected trithiocarbonates on histone H3 S^{10} phosphorylation. In contrast to the study by Li et al. using hydroxamates like TSA, compounds **8c** and **18a** induced histone H3 S^{10} phosphorylation and in parallel H3 K$^{1-20}$ hyperacetylation (Figure 6B). Compound **22** behaved as expected, only inducing histone H3 hyperacetylation, whereas compound **2** showed the opposite

effect. All analogues induced α-tubulin hyperacetylation as evidence for cellular HDAC6 inhibition. Interestingly, this α-tubulin hyperacetylation was strongly reduced for compounds **2** and **18a** at the 10 μM concentration, inducing strong histone H3 S^{10} phosphorylation and most likely mitotic arrest. From these experiments, we conclude that selected trithiocarbonate analogues show unique cellular properties with similarities to antimitotic agents like taxol, arresting RKO colon carcinoma cells transiently in mitosis before execution of apoptosis. We hypothesize that a new lysine specific protein deacetylase or a hypothetical mitotic HDAC complex are targeted by these antimitotic trithiocarbonate analogues.

Experimental Section

Biological Methods. Biochemical HDAC Assay. HDAC activity was isolated from HeLa nuclear extracts according to a method originally described by Dignam et al.[31] Mass cultures of HEK293 cell lines with stable expression of human rHDAC1 and rHDAC6 (kindly provided by E.Verdin, Gladstone Institute for Immunology, San Francisco) were lysed and flag-tagged proteins purified by M2-agarose affinity chromatography (Sigma art. no. A-2220). Fractions from the purification were analyzed by Western blotting and for specific activity in the biochemical enzyme assay. The HDAC enzyme activity assay was done essentially as described.[14,32] About 4 ng/well HDAC1 or 3 ng/well HDAC6 were incubated with 6 or 10 μM Ac-NH-GGK(Ac)-AMC, respectively, as substrate for 2 or 3 h at 30 °C. For enzyme kinetic studies, rHDAC1 (specific activity 0.39 μmol/min/mg) and rHDAC6 (specific activity 0.78 μmol/min/mg) enzymes were incubated with different substrate and inhibitor concentrations. For both enzymes, the substrate Ac-GGK(Ac)-AMC was used up to 100 μM final concentration (K_m values of 32.3 and 7.3 μM for rHDAC1 and rHDAC6, respectively). For trithiocarbonate analogues, the concentrations were selected based on IC$_{50}$ values, namely $^1/_4$, $^1/_2$, 1, 2, and 4 times the EC$_{50}$ concentration. Substrate concentration (mol/L) was plotted versus enzyme velocity (μmol/min), and K_i values were calculated from Lineweaver−Burk plots using GraphPad prism algorithms. A substrate competitive bindung mode is evident by a point of intersection on the *y*-axis.

Cellular Histone H3/Tubulin Hyperacetylation, p21, and Phosphohistone H3 Induction Assays. Histone H3 hyperacetylation was quantified using a single-cell based high content assay (HCS) format on the Cellomics "ArrayScan II" platform (Thermo Fisher Scientific, Waltham, MA) as described.[14] Briefly, HeLa cells in 96-well microtiter plates were treated with test compound for 24 h, fixed, permeabilized, and stained with a polyclonal rabbit antibody specific for histone H3K(Ac)$^{1-20}$ (Calbiochem, Darmstadt/Germany). Data analysis was done with the Cellomics algorithm "mitotic index", calculating normalized nuclear fluorescence intensity, correlating with the level of histone H3 hyperacetylation.

In parallel to the histone H3 hyperacetylation assay, the cellular efficacy and mode-of-action of HDAC inhibitors was studied in treated HeLa, RKO, or A549 cell lysates by Western blotting using antibodies specific for acetylated or phosphorylated histone H3, acetylated α-tubulin, and p21^{waf1}. After treatment with compound for 24 h, cells were lysed (50 mM Tris HCl pH 8, 150 mM NaCl, 1 v/v NP-40, 0.5% w/v Na-desoxycholate, 0.2% w/v disodium-dodecylsulfate (SDS), 0.02% NaN$_3$, 1 mM Na-vanadate, 20 mM NaF, 100 μg/mL PMSF, protease inhibitor mix/Roche and 50U/mL benzonase) and respective equal amounts of protein separated by SDS-PAGE before transfer to polyvinylidendifluoride/PVDF membrane (Biorad) by semidry blotting. The following antibodies were used for Western blot analysis: Acetylated histone H3 K$^{1-20}$ (Calbiochem no. 382158), histone H3 (Cell Signaling no. 9715), phosphorylated histone H3 S^{10} (Cell Signaling no. 9701), p21 (Santa Cruz no. SC-397), acetylated α-tubulin (Sigma T-6793), and β-actin (Sigma A-5441).

Cellular HDAC Enzymatic Activity Assay. A 96-well micro-titer plate assay was established using Boc-K(Ac)-AMC as substrate

as described recently.[27] HeLa cells were seeded into white 96-well tissue culture plates at a density of 5×10^3 cells/well and cultivated for 24 h under standard cell culture conditions. After treatment with trithiocarbonate analogues for 3 h, 10 μL/well of a 2 mM stock solution of the substrate Boc-K(Ac)-AMC in culture medium were added and incubation continued for additional 3 h before addition of 100μL/well lysis/developer buffer mix (50 mM Tris HCl pH 8.0, 137 mM NaCl, 2.7 mM KCl, 1 mM MgCl$_2$, 1 vol % Nonidet P40, 2.0 mg/mL trypsin, 10 μM TSA). After final incubation for 3 h under cell culture conditions, AMC fluorescence was measured at an excitation of λ = 355 nm and emission of λ = 460 nm on the Perkin-Elmer Wallac Victor II V multilabel plate reader (Perkin-Elmer, Wellesley, MA).

Proliferation Assay and Tumor Cell Lines. The antiproliferative activity of trithiocarbonate analogues on diverse tumor cell lines was evaluated by using the Alamar Blue (Resazurin) cell viability assay.[28] Cells were seeded into 96-well flat bottom plates at respective densities to allow proliferation during 72 h cultivation with test compound. The assay was done essentially done as described.[29] The following human tumor cell lines were used: H460 (nonsmall cell lung cancer, ATCC HTB-177), A549 (nonsmall cell lung cancer, ATCC CCL-185), MCF7 (breast carcinoma, ATCC HTB-22), MDA-MB468 (breast carcinoma, ATCC HTB-132), MDA-MB435 (HTB129), MDA-MB231 (breast carcinoma, ATCC HTB-26), SK-BR-3 (breast carcinoma, ATCC HTB-30), SK-OV-3 (ovarian carcinoma, ATCC HTB-77), HCT-15 (colon carcinoma, ATCC CCL-225), PC3 (prostate carcinoma, ATCC CRL-1435), AsPC1 (pancreatic carcinoma, ATCC CRL-1682), HeLa (cervical carcinoma, ATCC CCL-2), Cal27 (tongue carcinoma, ATCC CRL-2095), A-431 (vulva carcinoma, ATCC CRL-2592), Hec1A (endometrial carcinoma, ATCC HTB-112), Saos-2 (osteosarcoma, ATCC HTB-85), U87MG (glioblastoma, ATCC HTB-14), K562 (chronic myeloid leukemia, DSMZ ACC 10), EOL1 (acute hypereosinophilic myeloid leukemia, DSMZ ACC386), and CCRF-CEM and CCRF-CEM VCR1000 (acute lymphoblastic T-cell leukemia sensitive and resistant toward vincristine and DSMZ 240).[33] The human colon adenocarcinoma cell line RKO and transfectant RKOp21^{waf1} were described recently.[34] p21^{waf1} expression was induced by treatment with 10 μM ponasterone A for 24 h and RKO cells with/without p21^{waf1} expression (2×10^4 cells/well induced, 6×10^3 cells/well not induced) were treated with the compounds as described.[29] All cell lines were cultivated at 37 °C, 5% CO$_2$ in medium as stated on the ATCC, DSMZ, and ECACC information sheets or as published.

Flow Cytometric Analysis. RKO colon carcinoma cells were seeded at 5×10^5 cells/10 cm cell culture dish 24 h before treatment to allow logarithmic proliferation during the experiment. After about 24 h, cells were treated with test compound for 24 and 48 h. Further procedure and flow cytomteric analysis was done as described using the Becton Dickinson FACS Canto device.[29]

Chemical Procedures. Reagents and solvents were used as purchased from the supplier. Usually, reactions were run under nitrogen atmosphere (N$_2$-balloon). Unless otherwise stated, preparations were typically performed on a 0.5 mmol scale. NMR spectra were recorded on a Bruker DPX200, a Bruker AV400, a Bruker AVII300, or on a Bruker AV600 in the solvent given. Mass spectra were recorded on a LCQ classic by Thermofinnigan and GC-MS spectra on a Trace MS (Thermofinnigan). Reaction progress was monitored by analytical LC-MS on an Agilent 1100.

Preparation of Ethyl Trithiocarbonates (Procedure A). A 0.5 M solution of sodium ethyl trithiocarbonate was prepared by adding carbon disulfide (1.3 equiv) to a suspension of sodium thioethanolate (1.2 equiv) in tetrahydrofuran at room temperature and stirring of the resulting yellow solution for 30 min. Phenacyl bromide or chloride (1.0 equiv) was dissolved in ethyl acetate at room temperature and a 0.5 M solution of sodium ethyl trithiocarbonate (1.2 equiv) was added via syringe. After 1−3 h, the reaction mixture was diluted with half-saturated brine, and the aqueous phase was extracted with dichloromethane three times. The organic layer was dried via filtration through IST phase separator cartridge and evaporated to leave a yellowish residue, which was purified by chromatography (silica, hexanes to hexanes/ethyl acetate 1:1) providing the title compounds.

Ethyl 2-(4-Methylphenyl)-2-oxoethyl Trithiocarbonate (2). 2 was prepared from 2-bromo-1-*p*-tolyl-ethanone using general procedure A; yellow solid (59%). ^{1}H NMR (DMSO-*d*$_6$, 400 MHz, rt) δ (ppm) : 7.94 (d, *J* = 8.2 Hz, 2H), 7.37 (d, *J* = 8.2 Hz, 2H), 5.10 (s, 2H), 3.38 (q, *J* = 7.3 Hz, 2H), 2.38 (s, 3H), 1.29 (t, *J* = 7.3 Hz, 3H). LC-MS (*m/e*): 271 [M + H]$^+$.

Ethyl 2-(4-Methoxyphenyl)-2-oxoethyl Trithiocarbonate (3a). 3a was prepared from 2-bromo-1-(4-methoxy-phenyl)-ethanone using general procedure A; yellow solid (79%). ^{1}H NMR (DMSO-*d*$_6$, 200 MHz, rt) δ (ppm): 8.02 (d, *J* = 8.9 Hz, 2H), 7.08 (d, *J* = 8.9 Hz, 2H), 5.08 (s, 2H), 3.86 (s, 3H), 3.38 (q, *J* = 7.4 Hz, 2H), 1.29 (t, *J* = 7.4 Hz, 3H). LC-MS (*m/e*): 287 [M + H]$^+$.

2-(4-Methoxyphenyl)-2-oxoethyl Dithiobutyrate (3b). A solution of 1-propylmagnesium bromide (1.0 equiv) in diethyl ether (2 M) was diluted with tetrahydrofuran (0.2 M) and cooled to −20 °C under a nitrogen atmosphere. Copper iodide (0.1 equiv) and, 5 min later, carbon disulfide (1.0 equiv) was added to yield a dark solution. After 20 min, 2-bromo-1-(4-methoxy-phenyl)-ethanone was added and the mixture was stirred for 5 min. The reaction mixture was then poured into brine and the aqueous phase was extracted with ethyl acetate. The organic phases were dried over anhydrous magnesium sulfate and evaporated. Chromatographical purification (silica, hexanes/ethyl acetate) provided **3b** as pale-yellow oil (13%). ^{1}H NMR (DMSO-*d*$_6$, 200 MHz, rt) δ (ppm): 8.01 (d, *J* = 9.6 Hz, 2H), 6.97 (d, *J* = 9.6 Hz, 2H), 4.76 (s, 2H), 3.89 (s, 3H), 3.06 (t, *J* = 7.5 Hz, 2H), 1.92 (quin, *J* = 7.2 Hz, 2H), 1.00 (t, *J* = 7.4 Hz, 3H). LC-MS (*m/e*): 269 [M + H]$^+$.

***O*-Ethyl *S*-2-(4-methoxy-phenyl)-2-oxoethyl Dithiocarbonate (3c).** A 0.5 M solution of sodium ethanolate (1.0 equiv) was added carbon disulfide (1.15 equiv) in tetrahydrofuran at room temperature, and the resulting solution was stirred for 30 min. 4-Methoxy-phenacylbromide (1.0 equiv) was added via syringe. After 1 h, the reaction mixture was diluted with half-saturated brine and the aqueous phase was extracted with dichloromethane three times. The organic layer was dried via filtration through an IST phase separator cartridge and evaporated to leave a yellowish residue, which was purified by chromatography (silica gel, hexanes to hexanes/ethyl acetate 1:1), providing **3c** as whitish solid (93%). ^{1}H NMR (DMSO-*d*$_6$, 200 MHz, rt) δ (ppm): 8.00 (d, *J* = 8.9 Hz, 2H), 7.08 (d, *J* = 8.9 Hz, 2H), 4.88 (s, 2H), 4.22 (q, *J* = 7.1 Hz, 2H), 3.86 (s, 3H), 1.21 (t, *J* = 7.3 Hz, 3H). GC-MS: 271 [M]$^+$, 135 [M-119]$^+$.

***N*-Ethyl *S*-2-(4-Methoxy-phenyl)-2-oxoethyl Dithiocarbamate (3d).** A solution of 2-mercapto-1-(4-methoxy-phenyl)-ethanone **4** (1.0 equiv) in tetrahydrofuran (0.2 M) was treated with ethylthioisocyanate (1.2 equiv) at 0 °C. The reaction mixture was allowed to warm to rt overnight, poured into saturated sodium bicarbonate solution, and extracted with ethyl acetate. The organic phases were dried over anhydrous magnesium sulfate and evaporated to yield **3i** as pale-white powder (71%). **3d** exists in solution in equilibrium with a cyclized hemiaminal with the ratio being dependent on the solvent. ^{1}H NMR (DMSO-*d*$_6$, 400 MHz, rt) open chain δ (ppm): 10.05 (bs, 1H), 8.01 (d, *J* = 8.9 Hz, 2H), 7.08 (d, *J* = 8.9 Hz, 2H), 4.84 (s, 2H), 3.86 (s, 3H), 3.66 (m, 2H), 1.15 (t, *J* = 7.2 Hz, 3H). Cyclized hemiaminal δ (ppm): 7.57 (s, 1H), 7.36 (d, *J* = 8.8 Hz, 2H), 6.99 (d, *J* = 8.8 Hz, 2H), 3.69 (s, 3H), 3.57 (s, 2H), 3.57 (qd, *J* = 7.1, 6.5 Hz, 1H), 3.22 (qd, *J* = 7.1, 6.5 Hz, 1H), 0.98 (t, *J* = 7.1 Hz, 2H). LC-MS (*m/e*): 270 [M + H]$^+$.

***S*-Ethyl *O*-2-(4-Methoxy-phenyl)-2-oxoethyl Dithiocarbonate (3e).** A mixture of 2-hyxdroxy-1-(4′-methoxyphenyl)-ethanone (**6**) (0.50 g, 3.0 mmol), ethyleneglycol (4 mL), and amberlyst 15 (0.80 g) in benzene was refluxed in a Dean−Stark apparatus for 3 h. The mixture was extracted with saturated bicarbonate solution and brine, and the solvents were removed under reduced pressure to leave the product, which was used without further purification. A solution of the dioxolane (0.6 g, 2.9 mmol) in tetrahydrofuran (19 mL) was added dropwise to a suspension of NaH (60% in mineral oil, 0.28 g, 7.1 mmol) and imidazole (10 mg) in tetrahydrofuran (25 mL) at 0 °C. After stirring for 30 min at rt, carbon

disulfide (430 μL, 7.1 mmol) was added. The mixture was again stirred for 30 min, before ethyl iodide (575 μL, 7.1 mmol) was added and the mixture was stirred for further 1 h. Then the reaction mixture was poured onto ice and extracted with ethyl acetate. The organic phases were dried over anhydrous magnesium sulfate and evaporated. The residue was purified using chromatography (silica, dichloromethane/hexanes 4:1) to yield the product as whitish solid (0.65 g, 72%). The mixture of the resulting dioxolane (0.30 g, 0.95 mmol) in tetrahydrofuran/H_2O (3:1, 4 mL) was treated with a few drops of conc HCl and stirred at 60 °C for 4 h. The reaction mixture was poured into water and extracted with dichloromethane. The organic phases were dried over anhydrous magnesium sulfate and evaporated. The residue was purified using chromatography (silica, dichloromethane/hexanes 3:2) to yield **3e** as a colorless solid (0.20 g, 78%). ^{1}H NMR (CDCl_3, 200 MHz, rt) δ (ppm): 7.92 (d, $J = 9.2$ Hz, 2H), 6.97 (d, $J = 9.2$ Hz, 2H), 5.84 (s, 2H), 3.88 (s, 3H), 3.19 (q, $J = 7.1$ Hz, 2H), 1.39 (t, $J = 7.1$ Hz, 3H). LC-MS (m/e): 271 [M + H]$^+$.

Preparation of Trithiocarbonates (Procedure B). A 0.5 M solution of alkyl sodium trithiocarbonate is prepared by adding carbon disulfide (1.15 equiv) to a suspension of the requisite sodium thiolate (1.0 equiv) in tetrahydrofuran at room temperature and stirring of the resulting yellow solution for 30 min. Phenacyl bromide (1.0 equiv) was dissolved in ethyl acetate at room temperature, and a 0.5 M solution of sodium alkyl trithiocarbonate (1.2 equiv) was added as syringe. After 1−3 h, the reaction mixture was diluted with half-saturated brine and the aqueous phase was extracted with dichloromethane three times. The organic layer was dried via filtration through an IST phase separator cartridge and evaporated to leave a yellowish residue, which was purified by chromatography (silica gel, hexanes to hexanes/ethyl acetate 1:1), providing the title compounds.

Preparation of Trithiocarbonates Using PTT in Situ Bromination, Method a (Procedure C). A solution of phenylethanone **7** (1.0 equiv) in tetrahydrofuran (0.2−0.5 M) was treated with phenyltrimethylammonium tribromide (PTT, 1.1 equiv) at rt. The mixture was stirred at rt until the reaction was complete (TLC control and appearance of a white precipitate, 3 min to 16 h). To this reaction mixture, a 0.5 M solution of sodium ethyl trithiocarbonate (1.5−3 equiv) was added via syringe. After completion of the reaction, the reaction mixture was diluted with half-saturated brine and the aqueous phase was extracted with dichloromethane three times. The organic layer was dried via filtration through an IST phase separator cartridge and evaporated to leave a yellowish residue, which was purified by chromatography (silica, hexanes to hexanes/ethyl acetate 1:1), providing the title compounds.

2-(4-Acetylamino-phenyl)-2-oxoethyl Ethyl Trithiocarbonate (8a). 8a was prepared from N-(4-acetyl-phenyl)-acetamide according to general procedure C; yellow solid (53%). ^{1}H NMR (DMSO-d_6, 200 MHz, rt) δ (ppm): 10.30 (s, 1H), 8.03 (d, $J = 8.7$ Hz, 2H), 7.76 (d, $J = 8.7$ Hz, 2H), 5.08 (s, 2H), 3.39 (q, $J = 7.4$ Hz, 2H), 2.10 (s, 3H), 1.29 (t, $J = 7.4$ Hz, 3H). LC-MS (m/e): 314 [M + H]$^+$.

O-Ethyl S-2-(4-Acetamido-phenyl)-2-oxoethyl Dithiocarbonate (8c). Ethyl chloroformate (210 μL, 2.2 mmoL) was added a solution of 2-mercapto-1-(4-methoxy-phenyl)-ethanone (365 mg, 2.0 mmol) in 4 mL of tetrahydrofuran at rt. Diisopropylethylamine (346 μL, 2.5 mmol) was added, and the mixture was stirred overnight. The reaction mixture was treated with half-saturated brine, and the aqueous phase was extracted with ethyl acetate. The organic phases were dried over anhydrous magnesium sulfate and evaporated. The residue was purified using rotating preparative thin layer chromatography (hexanes/ethyl acetate gradient) to yield **8c** as whitish solid (93%). ^{1}H NMR (DMSO-d_6, 200 MHz, rt) δ (ppm): 8.00 (d, $J = 8.9$ Hz, 2H), 7.08 (d, $J = 8.9$ Hz, 2H), 4.53 (s, 2H), 4.22 (q, $J = 7.1$ Hz, 2H), 3.86 (s, 3H), 1.21 (t, $J = 7.3$ Hz, 3H). GC-MS (m/e): 254 [M]$^+$, 135 [M-119]$^+$.

2-(3-Acetylamino-phenyl)-2-oxoethyl Ethyl Trithiocarbonate (8e). 8e was prepared from N-(3-acetyl-phenyl) acetamide according to procedure C; yellow solid (70%). ^{1}H NMR (DMSO-d_6, 400 MHz, rt) δ (ppm): 10.15 (s, 1H), 8.19 (s, 1H), 7.90 (d, $J =$

8.1 Hz, 1H), 7.77 (d, $J = 7.9$ Hz, 1H), 7.50 (d, $J = 7.0$ Hz, 1H), 5.10 (s, 2H), 3.39 (q, $J = 7.4$ Hz, 2H), 2.07 (s, 3H), 1.29 (t, $J = 7.3$ Hz, 3H). LC-MS (m/e): 314 [M + H]$^+$.

2-[4-(Acetylamino-methyl)-phenyl]-2-oxoethyl Ethyl Trithiocarbonate (8g). 8g was prepared from N-(4-acetyl-benzyl)-acetamide according to general procedure C; yellow solid (70%). ^{1}H NMR (DMSO-d_6, 200 MHz, rt) δ (ppm): 8.43 (t, $J = 6.0$ Hz, 1H), 8.00 (d, $J = 8.3$ Hz, 2H), 7.42 (d, $J = 8.3$ Hz, 2H), 5.10 (s, 2H), 4.34 (d, $J = 6.0$ Hz, 2H), 3.38 (q, $J = 7.4$ Hz, 2H), 1.90 (s, 3H), 1.29 (t, $J = 7.4$ Hz, 3H). LC-MS (m/e): 328 [M + H]$^+$.

Ethyl 2-(4-Methanesulfonylamino-phenyl)-2-oxoethyl Trithiocarbonate (8h). 8h was prepared from 2-chloro-1-(4-methane-sulfonylamino-phenyl)-ethanone using general procedure A; yellow oil (64%). ^{1}H NMR (DMSO-d_6, 200 MHz, rt) δ (ppm): 10.35 (s, 1H), 8.04 (d, $J = 8.8$ Hz, 2H), 7.32 (d, $J = 8.8$ Hz, 2H), 5.08 (s, 2H), 3.38 (q, $J = 7.3$ Hz, 2H), 3.14 (s, 3H), 1.29 (t, $J = 7.4$ Hz, 3H). LC-MS (m/e): 350 [M + H]$^+$.

Preparation of Arylamide Trithiocarbonates (Procedure D). A solution of the acetyl-aryl carboxylic acid (1.0 equiv) in tetrahydrofuran (0.3 M) was cooled to 0 °C, then isobutyl chloroformate (1.1 equiv) and N-methyl-morpholine (1.05 equiv) were added and the mixture was stirred for 45 min. The corresponding amine (1.2 equiv) was added, and the mixture was allowed to warm to rt slowly. After 18 h, phenyltrimethylammonium tribromide (PTT, 1.1 equiv) was added and the mixture was stirred at rt (1−18 h) until the orange solution became colorless and a white precipitate was observed. A solution of sodium ethyl trithiocarbonate (0.5 M in tetrahydrofuran, 2.0 equiv) was added and the mixture was stirred again for 2−18 h. After completion of the reaction, the reaction mixture was diluted with half-saturated brine, and the aqueous phase was extracted with dichloromethane. The organic layer was evaporated to leave a yellowish residue, which was purified either by chromatography (silica, hexanes/ethyl acetate gradient) or by washing the solid with a little ethyl acetate, providing the title compound as a pale-yellow solid.

Ethyl 2-oxo-2-(3-Phenylcarbamoyl-phenyl)-ethyl Trithiocarbonate (12aa). 12aa was prepared from aniline and 3-acetyl-benzoic acid according to general procedure D; yellow solid (18%). ^{1}H NMR (DMSO-d_6, 400 MHz, rt) δ (ppm): 10.45 (s, 1H), 8.58 (s, 1H), 8.27 (t, $J = 6.3$ Hz, 2H), 7.79 (d, $J = 7.7$ Hz, 2H), 7.75 (t, $J = 7.8$ Hz, 1H), 7.39 (t, $J = 7.6$ Hz, 2H), 7.14 (t, $J = 7.4$ Hz, 1H), 5.23 (s, 2H), 3.40 (q, $J = 7.4$ Hz, 2H), 1.30 (t, $J = 7.4$ Hz, 3H). LC-MS (m/e): 376 [M + H]$^+$.

Ethyl 2-oxo-2-(4-Phenylcarbamoyl-phenyl)-ethyl Trithiocarbonate (12ab). 12ab was prepared from aniline and 4-acetyl-benzoic acid according to general procedure D; yellow solid (30%). ^{1}H NMR (DMSO-d_6, 200 MHz, rt) δ (ppm): 10.45 (s, 1H), 8.19 (d, $J = 8.5$ Hz, 2H), 8.10 (d, $J = 8.5$ Hz, 2H), 7.80 (d, $J = 7.6$ Hz, 2H), 7.38 (t, $J = 7.6$ Hz, 2H), 7.13 (t, $J = 7.3$ Hz, 1H), 5.18 (s, 2H), 3.39 (q, $J = 7.3$ Hz, 2H), 1.30 (t, $J = 7.3$ Hz, 3H). LC-MS (m/e): 376 [M + H]$^+$.

Preparation of Pyrimidylamide Trithiocarbonates, Method c (Procedure E). A solution of the 1-(hetero)aryl-ethanone (1.0 equiv) in tetrahydrofuran (0.08 M) was treated with a solution of sodium hexamethyldisilazide (1.1−2.2 equiv) at −78 °C and then stirred for 0.5 h. Trimethylsilylchloride (1.1−2.2 equiv) was added, and the mixture was stirred for 1 h at −78 °C. After the addition of a solution of bromine (1.0 equiv) in tetrahydrofuran (0.5 M), the mixture was stirred again for 1 h at −78 °C and then allowed to warm to rt. A solution of sodium ethyl trithiocarbonate (0.5 M in tetrahydrofuran, 3.0 equiv) was added, and the mixture was stirred again for 2−18 h. The reaction mixture was poured into a 2:1 mixture of 5% sodium bicarbonate and 5% sodium bisulfite solution and extracted with ethyl acetate. The organic phases were washed with brine and dried with sodium sulfate. Evaporation in vacuo gave an oily residue, which was purified by chromatography (silica, hexanes/ethyl acetate gradient) or by preparative HPLC (acetonitrile/water gradient), providing the title compounds.

2-(3-Benzylcarbamoyl-phenyl)-2-oxoethyl Ethyl Trithiocarbonate (12al). 12al was prepared from benzylamine and 3-acetyl-benzoic acid according to general procedure D; yellow solid (63%).

^{1}H NMR (DMSO-d_6, 400 MHz, rt) δ (ppm): 9.30 (t, J = 5.9 Hz, 1H), 8.56 (s, 1H), 8.21 (d, J = 7.8 Hz, 2H), 7.70 (t, J = 7.7 Hz, 1H), 7.36−7.33 (m, 4H), 7.29−7.23 (m, 1H), 5.19 (s, 2H), 4.53 (d, J = 5.9 Hz, 2H), 3.38 (q, J = 7.4 Hz, 2H), 1.29 (t, J = 7.4 Hz, 3H). LC-MS (m/e): 390 [M + H]$^+$.

2-(4-Benzylcarbamoyl-phenyl)-2-oxoethyl Ethyl Trithiocarbonate (12am). 12am was prepared from benzylamine and 4-acetyl-benzoic acid according to general procedure D; yellow solid (49%). ^{1}H NMR (DMSO-d_6, 200 MHz, rt) δ (ppm): 9.23 (t, J = 5.9 Hz, 1H), 8.16 (d, J = 8.5 Hz, 2H), 8.04 (d, J = 8.5 Hz, 2H), 7.36−7.23 (m, 5H), 5.16 (s, 2H), 4.50 (d, J = 5.9 Hz, 2H), 3.38 (q, J = 7.4 Hz, 2H), 1.29 (t, J = 7.4 Hz, 3H). LC-MS (m/e): 390 [M + H]$^+$.

Preparation of Pyrimidylamide Trithiocarbonates, Method d (Procedure F). A solution of 4-(2-bromo-acetyl)-benzenesulfonic acid chloride (1.0 equiv) in tetrahydrofuran (0.08 M) was treated with the requisite arylamine (1.1−2.2 equiv) and diisopropylethyl-lamine (1.1 equiv) at rt and then stirred for 0.5 h. A solution of sodium ethyl trithiocarbonate (0.5 M in tetrahydrofuran, 3.0 equiv) was added, and the mixture was stirred again for 18 h. The reaction mixture was poured into a 2:1 mixture of 5% sodium bicarbonate and extracted with ethyl acetate. The organic phases were washed with brine and dried with sodium sulfate. Evaporation in vacuo gave an oily residue, which was purified by chromatography (silica, hexanes/ethyl acetate gradient) or by preparative HPLC (acetonitrile/water gradient), providing the title compounds.

Ethyl 2-oxo-2-[5-((S)-1-phenyl-ethylcarbamoyl)-thiophen-2-yl]-ethyl Trithiocarbonate (16b). 16b was prepared from (S)-1-phenyl-ethylamine and 5-acetyl-thiophene-2-carboxylic acid according to general procedure E; yellow solid (6%). ^{1}H NMR (DMSO-d_6, 400 MHz, rt) δ (ppm): 9.15 (d, J = 8.0 Hz, 1H), 8.18 (d, J = 4.0 Hz, 1H), 8.01 (d, J = 4.0 Hz, 1H), 7.40 (d, J = 7.2 Hz, 2H), 7.35 (t, J = 7.2 Hz, 2H), 7.25 (t, J = 7.1 Hz, 1H), 5.13 (quint, J = 7.4 Hz, 1H), 5.07 (s, 2H), 4.48 (d, J = 6.0 Hz, 2H), 3.38 (q, J = 7.3 Hz, 2H), 1.50 (d, J = 7.1 Hz, 3H), 1.29 (t, J = 7.4 Hz, 3H). LC-MS (m/e): 410 [M + H]$^+$.

Ethyl 2-oxo-2-[5-((R)-1-Phenyl-ethylcarbamoyl)-thiophen-2-yl]-ethyl Trithiocarbonate (16c). 16c was prepared from (R)-1-phenyl-ethylamine and 5-acetyl-thiophene-2-carboxylic acid according to general procedure D; yellow solid (44%). ^{1}H NMR (DMSO-d_6, 400 MHz, rt) δ (ppm): 9.15 (d, J = 8.0 Hz, 1H), 8.18 (d, J = 4.0 Hz, 1H), 8.01 (d, J = 4.0 Hz, 1H), 7.40 (d, J = 7.2 Hz, 2H), 7.35 (t, J = 7.2 Hz, 2H), 7.25 (t, J = 7.1 Hz, 1H), 5.13 (quint, J = 7.4 Hz, 1H), 5.07 (s, 2H), 4.48 (d, J = 6.0 Hz, 2H), 3.38 (q, J = 7.3 Hz, 2H), 1.50 (d, J = 7.1 Hz, 3H), 1.29 (t, J = 7.4 Hz, 3H). LC-MS (m/e): 410 [M + H]$^+$.

2-[5-(3,5-Dimethyl-benzylcarbamoyl)-thiophen-2-yl]-2-oxoet-hyl Ethyl Trithiocarbonate (16d). 16d was prepared from 3,5-dimethyl-benzylanime and 5-acetyl-thiophene-2-carboxylic acid according to general procedure D; yellow solid (21%). ^{1}H NMR (DMSO-d_6, 400 MHz, rt) δ (ppm): 9.27 (t, J = 5.9 Hz, 1H), 8.16 (d, J = 4.1 Hz, 1H), 7.90 (d, J = 4.1 Hz, 1H), 6.92 (s, 2H), 6.90 (s, 1H), 5.07 (s, 2H), 4.40 (d, J = 5.9 Hz, 2H), 3.39 (q, J = 7.4 Hz, 2H), 2.25 (s, 6H), 1.29 (t, J = 7.4 Hz, 3H). LC-MS (m/e): 424 [M + H]$^+$.

Preparation of Thiophenylmethylamide Trithiocarbonates (Procedure G). A solution of [5-(2-chloro-ethanoyl)-thiophen-2-yl]-acetic acid (1.0 equiv) in tetrahydrofuran (0.2 M) was cooled to 0 °C, then isobutyl chloroformate (1.2 equiv) and N-methyl-morpholine (1.2 equiv) were added and the mixture was stirred for 45 min. The corresponding amine (1.2 equiv) was added, and the mixture was allowed to warm to rt slowly. After 1 h, a solution of sodium ethyl trithiocarbonate (0.5 M in tetrahydrofuran, 1.5 equiv) was added and the mixture was stirred again for 18 h. After completion of the reaction, the reaction mixture was diluted with half-saturated brine and the aqueous phase was extracted with dichloromethane. The organic layer was evaporated to leave a yellowish residue, which was purified by chromatography (silica, hexanes/ethyl acetate gradient) followed by preparative HPLC (acetonitrile/water gradient), providing the title compound as a pale-yellow solid.

2-[5-(Benzylcarbamoyl-methyl)-thiophen-2-yl]-2-oxoethyl Eth-yl Trithiocarbonate (18a). 18a was prepared from benzylamine according to general procedure G; yellow solid (13%). ^{1}H NMR (DMSO-d_6, 200 MHz, rt) δ (ppm): 8.67 (t, J = 5.7 Hz, 1H), 8.00 (d, J = 3.8 Hz, 1H), 7.37−7.24 (m, 5H), 7.09 (d, J = 3.9 Hz, 1H), 5.01 (s, 2H), 4.20 (d, J = 5.8 Hz, 2H), 3.83 (s, 2H), 3.38 (q, J = 7.4 Hz, 2H), 1.29 (t, J = 7.3 Hz, 3H). LC-MS (m/e): 410 [M + H]$^+$.

Ethyl 2-oxo-2-{5-[(2-Phenoxy-ethylcarbamoyl)-methyl]-thio-phen-2-yl}-ethyl Trithiocarbonate (18d). 18d was prepared from 2-phenoxy-ethylamine according to general procedure G; yellow solid (17%). ^{1}H NMR (DMSO-d_6, 200 MHz, rt) δ (ppm): 8.46 (t, J = 5.5 Hz, 1H), 7.98 (d, J = 3.9 Hz, 1H), 7.29 (t, J = 8.1 Hz, 2H), 7.07 (d, J = 3.9 Hz, 1H), 6.97−6.91 (m, 3H), 5.00 (s, 2H), 4.00 (t, J = 5.5 Hz, 2H), 3.73 (s, 2H), 3.46 (t, J = 5.6 Hz, 2H), 3.38 (t, J = 7.4 Hz, 2H), 1.29 (t, J = 7.3 Hz, 3H). LC-MS (m/e): 440 [M + H]$^+$.

Preparation of Pyridinyl Acetylthiophenes (Procedure H). A solution of pyridinyl-bromide (1.0 equiv) and 5-acetyl-thienyl-2-boronic acid (1.05 equiv) in dioxane/water (10:1, 0.2 M) was charged with Pd(dppf)Cl$_2$ (0.01 equiv) and cesium carbonate (1.4 equiv), then purged with nitrogen and the mixture was stirred at 15 rt for 18 h. The reaction mixture was diluted with dichloromethane and filtered through a silica pad. Evaporation in vacuo and subsequent purification by flash chromatography (silica, hexanes/ethyl acetate gradient) yielded the desired product.

2-(5-{5-[(3-Amino-quinolinyl)-methyl]-pyridin-2-yl}-thiophen-2-yl)-2-oxoethyl Ethyl Trithiocarbonate (22). 2-(5-{5-[(3-amino-quinolinyl)-methyl]-pyridin-2-yl}-thiophen-2-yl)-ethanone (21a) was prepared from (4-bromo-benzyl)-quinolin-3-yl-amine according to procedure H; yellow solid (51%). ^{1}H NMR (DMSO-d_6, 400 MHz, rt) δ (ppm): 8.68 (d, J = 1.6 Hz, 1H), 8.56 (d, J = 2.8 Hz, 1H), 8.04 (d, J = 8.2 Hz, 1H), 7.95−7.91 (m, 2H), 7.87 (d, J = 4.1 Hz, 1H), 7.79 (d, J = 8.0 Hz, 1H), 7.62 (d, J = 7.8 Hz, 1H), 7.38 (t, J = 6.7 Hz, 1H), 7.34 (t, J = 6.7 Hz, 1H), 7.08 (d, J = 1.6 Hz, 1H), 6.99 (t, J = 4.0 Hz, 1H), 5.07 (s, 2H), 4.48 (t, J = 4.0 Hz, 2H), 2.55 (s, 3H). LC-MS (m/e): 360 [M + H]$^+$.

22 was prepared from 21a according to general procedure E: yellow solid (9%). ^{1}H NMR (DMSO-d_6, 400 MHz, rt) δ (ppm): 8.69 (s, 1H), 8.56 (d, J = 2.7 Hz, 1H), 8.18 (d, J = 4.1 Hz, 1H), 8.07 (d, J = 8.2 Hz, 1H), 7.95−7.91 (m, 2H), 7.79 (d, J = 7.9 Hz, 1H), 7.62 (d, J = 7.8 Hz, 1H), 7.38 (t, J = 6.7 Hz, 1H), 7.34 (t, J = 6.7 Hz, 1H), 7.09 (s, 1H), 6.98 (t, J = 6.0 Hz, 1H), 5.07 (s, 2H), 4.48 (t, J = 6.0 Hz, 2H), 3.39 (q, J = 7.4 Hz, 2H), 1.29 (t, J = 7.4 Hz, 3H). LC-MS (m/e): 496 [M + H]$^+$.

2-(5-(5-Amino-pyrid-2-yl)-thieno-2-yl)-2-oxoethyl Ethyl Trithio-carbonate (23). 2-(5-(5-Amino-pyrid-2-yl)-thieno-2-yl)-ethanone (21b) was prepared from 5-amino-2-bromo-pyridine according to general procedure H; yellowish solid (44%). ^{1}H NMR (DMSO-d_6, 400 MHz, rt) δ (ppm): 7.94 (d, J = 2.6 Hz, 1H), 7.85 (d, J = 4.0 Hz, 1H), 7.69 (d, J = 8.6 Hz, 1H), 7.53 (d, J = 4.1 Hz, 1H), 6.97 (dd, J = 8.6, 2.7 Hz, 1H), 5.78 (s, 2H), 2.56 (s, 3H). LC-MS (m/e): 219 [M + H]$^+$.

23 was prepared from 21b according to general procedure E; yellow solid (10%). ^{1}H NMR (DMSO-d_6, 400 MHz, rt) δ (ppm): 8.09 (d, J = 4.0 Hz, 1H), 7.95 (d, J = 2.6 Hz, 1H), 7.73 (d, J = 8.6 Hz, 1H), 7.59 (d, J = 4.1 Hz, 1H), 6.98 (dd, J = 8.5, 2.7 Hz, 1H), 5.77 (s, 2H), 5.03 (s, 2H), 3.39 (q, J = 7.4 Hz, 2H), 1.29 (t, J = 7.4 Hz, 3H). LC-MS (m/e): 355 [M + H]$^+$.

HPLC Purity. Purity of all compounds was determined by analytical HPLC using a HPLC equipment of the LiChroGraph series by Hitachi (pressure gradient pump L-7100), a reversed phase column by Waters (Xterra, 100 mm × 2.1 mm inner diameter), and as eluent a 10 mM ammoniumacetate/acetonitrile gradient (buffer to pH 7,4). The purity of the compounds was determined using a diode array detector (Hitachi L-7455, cell: 10 mm, 8 μL) at λ = 230−330 nm. All compounds possessed a purity of greater than 95% as determined as average value of two independent injections (see Table 5 for key compounds). Tracings of key compounds are given as Supporting Information.

Table 5. Purity of Key Compounds as Determined by Analytical HPLC

no.		purity (%)
2	ethyl 2-(4-methylphenyl)-2-oxoethyl trithiocarbonate	100/100
3a	ethyl 2-(4-methoxyphenyl)-2-oxoethyl trithiocarbonate	99.1/98.9
3b	2-(4-methoxyphenyl)-2-oxoethyl dithiobutyrate	96.0/95.9
3c	O-ethyl S-2-(4-methoxy-phenyl)-2-oxoethyl dithiocarbonate	97.8/98.1
3d	N-ethyl S-2-(4-methoxy-phenyl)-2-oxoethyl dithiocarbamate	96.8/96.8
3e	S-ethyl O-2-(4-methoxy-phenyl)-2-oxoethyl dithiocarbonate	98.3/98.1
8a	2-(4-acetylamino-phenyl)-2-oxoethyl ethyl trithiocarbonate	95.2/95.7
8c	O-ethyl S-2-(4-acetamido-phenyl)-2-oxoethyl dithiocarbonate	100/100
8e	2-(3-acetylamino-phenyl)-2-oxoethyl ethyl trithiocarbonate	96.7/95.9
8g	2-[4-(acetylamino-methyl)-phenyl]-2-oxoethyl ethyl trithiocarbonate	99.7/99.7
8h	ethyl 2-(4-methanesulfonylamino-phenyl)-2-oxoethyl trithiocarbonate	98.6/98.9
12aa	ethyl 2-oxo-2-(3-phenylcarbamoyl-phenyl)-ethyl trithiocarbonate	97.8/98.1
12ab	ethyl 2-oxo-2-(4-phenylcarbamoyl-phenyl)-ethyl trithiocarbonate	98.0/97.5
12al	2-(3-benzylcarbamoyl-phenyl)-2-oxoethyl ethyl trithiocarbonate	99.5/99.8
12am	2-(4-benzylcarbamoyl-phenyl)-2-oxoethyl ethyl trithiocarbonate	97.4/97.9
16b	ethyl 2-oxo-2-[5-((S)-1-phenyl-ethylcarbamoyl)-thiophen-2-yl]-ethyl trithiocarbonate	95.2/95.3
16c	ethyl 2-oxo-2-[5-((R)-1-phenyl-ethylcarbamoyl)-thiophen-2-yl]-ethyl trithiocarbonate	99.4/99.3
16d	2-[5-(3,5-dimethyl-benzylcarbamoyl)-thiophen-2-yl]-2-oxoethyl ethyl trithiocarbonate	96.5/97.0
18a	2-[5-(benzylcarbamoyl-methyl)-thiophen-2-yl]-2-oxoethyl ethyl trithiocarbonate	99.5/99.5
18d	ethyl 2-oxo-2-{5-[(2-phenoxy-ethylcarbamoyl)-methyl]-thiophen-2-yl}-ethyl trithiocarbonate	98.7/98.7
22	2-(5-{5-[(3-amino-quinolinyl)-methyl]-pyridin-2-yl}-thiophen-2-yl)-2-oxoethyl ethyl trithiocarbonate	95.7/95.7
23	2-(5-(5-amino-pyrid-2-yl)-thieno-2-yl)-2-oxoethyl ethyl trithiocarbonate	98.5/98.6

Supporting Information Available: All information about chemical synthesis and analytics of additional compounds as presented in the manuscript but not shown in the Experimental Section. This material is available free of charge via the Internet at http://pubs.acs.org.

References

(1) (a) Cohen, T.; Yao, T. P. AcK-Knowledge reversible acetylation. *Sci. STKE 3* **2004**, pe42. (b) Yang, X. J.; Seto, E. HATs and HDACs: from structure, function and regulation to novel strategies for therapy and prevention. *Oncogene* **2007**, *26*, 5310–5318.

(2) Strahl, B. D.; Allis, C. D. The language of covalent histone modifications. *Nature* **2000**, *403*, 41–45.

(3) (a) Zhang, K.; Dent, S. Y. J. Histone modifying enzymes and cancer: going beyond histones. *Cell. Biochem.* **2005**, *96*, 1137–1148. (b) Johnstone, R. W.; Licht, J. D. Histone deacetylase inhibitors in cancer therapy: is transcription the primary target? *Cancer Cell* **2003**, *4*, 13–18.

(4) (a) de Ruijter, A. J.; van Gennip, A. H.; Caron, H. N.; Kemp, S.; van Kuilenburg, A. B. Histone deacetylases (HDACs): characterization of the classical HDAC family. *J. Biochem.* **2003**, *370*, 737–749. (b) Bolden, J. E.; Peart, M. J.; Johnstone, R. W. Anticancer activities of histone deacetylase inhibitors. *Nat. Rev. Drug. Discovery* **2006**, *5*, 769–784.

(5) (a) Marks, P.; Rifkind, R. A.; Richon, V. M.; Breslow, R.; Miller, T.; Kelly, W. K. Histone deacetylases and cancer: causes and therapies. *Nat. Rev. Cancer* **2001**, *1*, 194–202. (b) Minucci, S.; Pelicci, P. G. Histone deacetylase inhibitors and the promise of epigenetic (and more) treatments for cancer. *Nat. Rev. Cancer* **2006**, *6*, 38–51. (c) Glozak, M. A.; Seto, E. Histone deacetylases and cancer. *Oncogene* **2007**, *26*, 5420–5432.

(6) Murata, T.; Kurokawa, R.; Krones, A.; Tatsumi, K.; Ishii, M.; Taki, T.; Masuno, M.; Ohashi, H.; Yanagisawa, M.; Rosenfeld, M. G.; Glass, C. K.; Hayashi, Y. Defect of histone acetyltransferase activity of the nuclear transcriptional coactivator CBP in Rubinstein–Taybi syndrome. *Hum. Mol. Genet.* **2001**, *10*, 1071–1076.

(7) Wang, J.; Hoshino, T.; Redner, R. L.; Kajigaya, S.; Liu, J. M. ETO, fusion partner in t(8;21) acute myeloid leukemia, represses transcription by interaction with the human N-CoR/mSin3/HDAC1 complex. *Proc. Natl. Acad. Sci. U.S.A.* **1998**, *95*, 10860–10865.

(8) Zhu, P.; Martin, E.; Mengwasser, J.; Schlag, P.; Janssen, K. P.; Göttlicher, M. Induction of HDAC2 expression upon loss of APC in colorectal tumorigenesis. *Cancer Cell* **2004**, *5*, 455–463.

(9) (a) Weichert, W.; Röske, A.; Gekeler, V.; Beckers, T.; Ebert, M.; Pross, M.; Dietel, M.; Denkert, C.; Röcken, C. Class I HDAC expression patterns are highly prognostic in human gastric cancer. *Lancet Oncology* **2008**, *9*, 139–148. (b) Weichert, W.; Röske, A.; Niesporek, S.; Noske, A.; Buckendahl, A. C.; Dietel, M.; Gekeler, V.; Boehm, M.; Beckers, T.; Denkert, C. Class I histone deacetylase expression has independent prognostic impact in human colorectal cancer: specific role of class I HDACs in vitro and in vivo. *Clin. Cancer. Res.* **2008**, *14*, 1669–1677. (c) Weichert, W.; Röske, A.; Gekeler, G.; Beckers, T.; Stephan, C.; Jung, K.; Niesporek, S.; Denkert, C.; Dietel, M.; Kristiansen, G. Expression, function and prognostic role of class I histone deacetylase isoforms in prostate cancer in vitro and in vivo. *Br. J. Cancer* **2008**, *98*, 604–610.

(10) (a) Yoo, C. B.; Jones, P. A. Epigenetic therapy of cancer: past, present and future. *Nat. Rev. Drug Discovery* **2006**, *5*, 37–50. (b) Riester, D.; Hildmann, C.; Schwienhorst, A. Histone deacetylase inhibitors-turning epigenic mechanisms of gene regulation into tools of therapeutic intervention in malignant and other diseases. *Appl. Microbiol. Biotechnol.* **2007**, *75*, 499–514.

(11) Sorbera, L. A. Epigenetic targets as an approach to cancer therapy and chemoprevention. *Drugs Future* **2006**, *31*, 335–344.

(12) (a) Miller, T. A.; Witter, D. J.; Belvedere, S. Histone Deacetylase Inhibitors. *J. Med. Chem.* **2003**, *46*, 5097–5116. (b) Hildmann, C.; Wegener, D.; Riester, D.; Hempel, R.; Schober, A.; Merena, J.; Guirato, L.; Guccione, S.; Nielsen, T. K.; Ficner, R.; Schwienhorst, A. Substrate and inhibitor specificity of class 1 and class 2 histone deacetylases. *J. Biotechnol.* **2006**, *124*, 258–270.

(13) (a) Finnin, M. S.; Donigian, J. R.; Cohen, A.; Richon, V. M.; Rifkind, R. A.; Marks, P. A.; Breslow, R.; Pavletich, N. P. Structures of a histone deacetylase homologue bound to the TSA and SAHA inhibitors. *Nature* **1999**, *401*, 188–193. (b) Somoza, J. R.; Skene, R. J.; Katz, B. A.; Mol, C.; Ho, J. D.; Jennings, A. J.; Luong, C.; Arvai, A.; Buggy, J. J.; Chi, El.; Tang, J.; Sang, B.-C.; Verner, E.; Wynands, R.; Leahy, E. M.; Dougan, D. R.; Snell, G.; Navre, M.; Knuth, M. W.; Swanson, R. V.; McRee, D. E.; Tari, L. W. Structural Snapshots of Human HDAC8 Provide Insights into the Class I Histone Deacetylases. *Structure* **2004**, *12*, 1325–1334.

(14) Beckers, T.; Burkhardt, C.; Wieland, H.; Gimmnich, P.; Ciossek, T.; Maier, T.; Sanders, K. Distinct pharmacological properties of 2nd generation HDAC inhibitors with the benzamide or hydroxamate head group. *Int. J. Cancer* **2007**, *121*, 1138–1148.

(15) Haggarty, S. J.; Koeller, K. M.; Wong, J. C.; Grozinger, C. M.; Schreiber, S. L. Domain-selective small-molecule inhibitor of histone deacetylase 6 (HDAC6)-mediated tubulin deacetylation. *Proc. Natl. Acad. Sci. U.S.A.* **2003**, *100*, 4389–4394.

(16) Hodawadekar, S. C.; Marmorstein, R. Chemistry of acetyl transfer by histone modifying enzymes: structure, mechanismand implications for effector design. *Oncogene* **2007**, *26*, 5528–5540.

(17) (a) Suzuki, T.; Miyata, N. Rational Design of Non-Hydroxamate Histone Deacetylase Inhibitors. *Mini-Rev. Med. Chem.* **2006**, *6*, 515–526. (b) Suzuki, T.; Miyata, N. Non-hydroxamate Histone Deacetylase Inhibitors. *Curr. Med. Chem.* **2005**, *12*, 2867–2880.

(18) (a) For recent studies on hydroxamtes and benzamides, see for instance Anandan, S.-K.; Ward, J. S.; Brokx, R. D.; Denny, T.; Bray, M. R.; Patel, D. V.; Xiao, X.-Y. Design and synthesis of thiazole-5-hydroxamic acids as novel histone deacetylase inhibitors. *Bioorg. Med. Chem. Lett.* **2007**, *17*, 5995–5999. (b) Moradei, O. M.; Mallais, T. C.; Frechette, S.; Paquin, I.; Tessier, P. E.; Leit, S. M.; Fournel, M.;

Bonfils, C.; Trachy-Bourget, M.-C.; Liu, J.; Yan, T. P.; Lu, A. H.; Rahil, J.; Wand, J.; Lefebvre, S.; Li, Z.; Vaisburg, A. F.; Bestermann, J. M. Novel Aminophenyl Benzamide-Type Histone Deacetylase Inhibitors with Enhanced Potency and Selectivity. *J. Med. Chem.* **2007**, *50*, 5543–5546. (c) Hamblett, C. L.; Methot, J. L.; Mampreian, D. M.; Sloman, D. L.; Stanton, M. G.; Kral, A. M.; Fleming, J. C.; Cruz, J. C.; Chenard, M.; Ozerova, N.; Hitz, A. M.; Wang, H.; Deshmukh, S. V.; Nazef, N.; Harsch, A.; Hughes, B.; Dahlberg, W. K.; Szewczak, A. A.; Middleton, R. E.; Mosley, R. T.; Secrist, J. P.; Miller, T. A. The discovery of 6-amino nicotinamides as potent and selective histone deacetylase inhibitors. *Bioorg. Med. Chem. Lett.* **2007**, *17*, 5300–5309.

(19) (a) Suzuki, T.; Kouketsu, A.; Matsuura, A.; Kohara, A.; Ninomiya, S.-i.; Kohda, K.; Miyata, N. Thiol-based SAHA analogues as potent histone deacetylase inhibitors. *Bioorg. Med. Chem. Lett.* **2004**, *14*, 3313–3317. (b) Nishino, N.; Jose, B.; Okamura, S.; Ebisusaki, S.; Kato, T.; Sumida, Y.; Yoshida, M. Cyclic Tetrapeptides Bearing a Sulfhydryl Group Potently Inhibit Histone Deacetylases. *Org. Lett.* **2003**, *5*, 5079–5082. (c) Itoh, Y.; Suzuki, T.; Kouketsu, A.; Suzuki, N.; Maeda, S.; Yoshida, M.; Nakagawa, H.; Miyata, N. Design, Synthesis, Structure−Selectivity Relationship, and Effect on Human Cancer Cells of a Novel Series of Histone Deacetylase 6-Selective Inhibitors. *J. Med. Chem.* **2007**, *50*, 5425–5438.

(20) Suzuki, T.; Nagano, Y.; Kouketsu, A.; Matsuura, A.; Maruyama, S.; Kurotaki, M.; Nakagawa, H.; Miyata, N. Novel Inhibitors of Human Histone Deacetylases: Design, Synthesis, Enzyme Inhibition, and Cancer Cell Growth Inhibition of SAHA-Based Non-hydroxamates. *J. Med. Chem.* **2005**, *48*, 1019–1032.

(21) Furumai, R.; Matsuyama, A.; Kobashi, N.; Lee, K-H.; Nishiyama, M.; Nakajima, H.; Tanaka, A.; Komatsu, Y.; Nishino, N.; Yoshida, M.; Horinouchi, S. FK228 (Depsipeptide) as a Natural Prodrug That Inhibits Class I Histone Deacetylases. *Cancer Res.* **2002**, *62*, 4916–4921.

(22) (a) Yurek-George, A.; Cecil, A. R. L.; Mo, A. H. K.; Shijun, W.; Rogers, H.; Habens, F.; Maeda, S.; Yoshida, M.; Packham, G.; Ganesan, A. The First Biologically Active Synthetic Analogues of FK228, the Depsipeptide Histone Deacetylase Inhibitor. *J. Med. Chem.* **2007**, *50*, 5720–5726. (b) Shivashimpi, G. M.; Amagai, S.; Kato, T.; Nishino, N.; Maeda, S.; Nishino, T. G.; Yoshida, M. Molecular design of histone deacetylase inhibitors by aromatic ring shifting in chlamydocin framework. *Bioorg. Med. Chem.* **2007**, *15*, 7830–7839.

(23) (a) Suzuki, T.; Hisakawa, S.; Itoh, Y.; Maruyama, S.; Kurotaki, M.; Nakagawa, H.; Miyata, N. Identification of a potent and stable antiproliferative agent by the prodrug formation of a thiolate histone deacetylase inhibitor. *Bioorg. Med. Chem. Lett.* **2007**, *17*, 1558–1561. (b) Suzuki, T.; Kouketsu, A.; Itoh, Y.; Hisakawa, S.; Maeda, S.; Yoshida, M.; Nakagawa, H.; Miyata, N. Highly Potent and Selective Histone Deacetylase 6 Inhibitors Designed Based on a Small-Molecular Substrate. *J. Med. Chem.* **2006**, *49*, 4809–4812.

(24) (a) Anandan, S.-K.; Ward, J. S.; Brokx, R. D.; Bray, M. R.; Patel, D. V.; Xiao, X.-X. Mercaptoamide-based non-hydroxamic acid type histone deacetylase inhibitors. *Bioorg. Med. Chem. Lett.* **2005**, *15*, 1969–1972. (b) Chen, B.; Petukhov, P. A.; Jung, M.; Velena, A.; Eliseeva, E.; Dritschilo, A.; Kozikowski, A. P. Chemistry and biology of mercaptoacetamides as novel histone deacetylase inhibitors. *Bioorg. Med. Chem. Lett.* **2005**, *15*, 1389–1392. (c) Suzuki, T.; Matsuura, A.; Kouketsu, A.; Nakagawa, H.; Miyata, N. Identification of a potent non-hydroxamate histone deacetylase inhibitor by mechanism-based drug design. *Bioorg. Med. Chem. Lett.* **2005**, *15*, 331–335.

(25) Gu, W.; Nusinzon, I.; Smith, R. D., Jr.; Horvarth, C. M.; Silverman, R. B. Carbonyl- and sulfur-containing analogs of suberoylanilide hydroxamic acid: Potent inhibition of histone deacetylases. *Bioorg. Med. Chem.* **2006**, *14*, 3320–3329.

(26) Dehmel, F.; Ciossek, T.; Maier, T.; Weinbrenner, S.; Schmidt, B.; Zoche, M.; Beckers, T. Trithiocarbonates−Exploration of a new head group for HDAC inhibitors. *Bioorg. Med. Chem. Lett.* **2007**, *17*, 4746–4752.

(27) Ciossek, T.; Julius, H.; Wieland, H.; Maier, T.; Beckers, T. A homogeneous cellular histone deacetylase assay suitable for compound profiling and robotic screening. *Anal. Biochem.* **2008**, *372*, 72–81.

(28) O'Brien, J.; Wilson, I.; Orton, T.; Pognan, F. Investigation of the Alamar Blue (resazurin) fluorescent dye for the assessment of mammalian cell cytotoxicity. *Eur. J. Biochem.* **2000**, *267*, 5421–5426.

(29) Mahboobi, S.; Sellmer, A.; Hocher, H.; Garhammer, C.; Pongratz, H.; Maier, T.; Ciossek, T.; Beckers, T. 2-Aroylindoles and 2-aroyl-benzofurans with *N*-hydroxyacrylamide substructures as a novel series of rationally designed histone deacetylase inhibitors. *J. Med. Chem.* **2007**, *50*, 4405–4418.

(30) Li, Y.; Kao, G. D.; Garcia, B. A.; Shabanowitz, J.; Hunt, D. F.; Qin, J.; Phelan, C.; Lazar, M. A. A novel histone deacetylase pathway regulates mitosis by modulating Aurora B kinase activity. *Genes Dev.* **2006**, *20*, 2566–2579.

(31) Dignam, J. D.; Lebovitz, R. M.; Roeder, R. G. Accurate transcription initiation by RNA polymerase II in a soluble extract from isolated mammalian nuclei. *Nucleic Acids Res.* **1983**, *11*, 1475–1489.

(32) Wegener, D.; Wirsching, F.; Riester, D.; Schwienhorst, A. A fluorogenic histone deacetylase assay well suited for high-throughput activity screening. *Chem. Biol.* **2003**, *10*, 61–68.

(33) Ise, W.; Heuser, M.; Sanders, K.; et al. P-Glycoprotein-associated resistance to taxol and taxotere and its reversal by dexniguldipine-HCl, dexverapamil-HCl, or cyclosporin A. *Int. J. Oncol.* **1996**, *8*, 951–956.

(34) Schmidt, M.; Lu, Y.; Liu, B.; Fang, M.; Mendelsohn, J.; Fan, Z. Differential modulation of paclitaxel-mediated apoptosis by p21waf1 and p27kip1. *Oncogene* **2000**, *19*, 2423–2429.

JM800093C